

GROUND STATE AND SADDLE POINT: MASSES AND DEFORMATIONS FOR EVEN-EVEN SUPERHEAVY NUCLEI WITH $98 \leq Z \leq 126$ AND $134 \leq N \leq 192$

M. Kowal^{a,*}, P. Jachimowicz^b, J. Skalski^a

^a*National Centre for Nuclear Research , Hoża 69, PL-00-681 Warsaw, Poland*

^b*Institute of Physics, University of Zielona Góra, Szafrana 4a, 65516 Zielona Góra, Poland*

Abstract

We determine ground-state and saddle-point shapes and masses of even-even superheavy nuclei in the range of proton numbers $98 \leq Z \leq 126$ and neutron numbers $134 \leq N \leq 192$. Our study is performed within the microscopic-macroscopic method. The Strutinsky shell and pairing correction is calculated for the deformed Woods-Saxon single-particle potential and the Yukawa-plus-exponential energy is taken as a smooth part. We use parameters of the model that were fitted previously to this region of nuclei. A high-dimensional deformation space, including nonaxial and reflection-asymmetric shapes, is used in the search for saddle points. Both ground-state and saddle-point shapes are found with the aid of the minimization procedure, with dynamical programming technique of search for saddle points. The results are collected in two tables. Calculated ground-state mass-excess, Q_α energies, total and macroscopic energies normalized to the macroscopic energy at the spherical shape, shell corrections (including pairing) and deformations are given for each nucleus in the table one. The second table gives the same properties, but at the saddle-point configuration. The obtained results are discussed and compared with available experimental data for alpha-decay energies (Q_α) and ground-state masses.

arXiv:1203.5013v1 [nucl-th] 22 Mar 2012

*Corresponding author.

Email address: E-mail: m.kowal@fuw.edu.pl (M. Kowal)

Contents

1. Introduction	2
2. Method	3
2.1. Macroscopic energy	3
2.2. Microscopic energy	5
2.2.1. Woods-Saxon potential	5
2.2.2. Shell correction	6
2.2.3. Pairing correlations	7
2.2.4. Pairing correction	8
3. Shape parametrization	9
4. Dynamic programming method	10
5. Numerical tests and and error checks	10
6. Discussion of the results	11
6.1. Ground state properties	11
6.1.1. Ground state shapes (deformations)	11
6.1.2. Ground state mass excess	12
6.1.3. Q-alpha energies	12
6.2. Saddle point properties	13
6.2.1. Saddle point shapes (deformations)	13
6.2.2. Saddle point mass excess - fission barriers	13
7. Summary	13
References	34
Tables	
1. Calculated Ground State Masses and Deformations.	23
2. Calculated Saddle Point Masses and Deformations.	29

1. Introduction

The uncharted region of the Z - N plane can answer many questions of fundamental importance for science: How many neutrons can be bound in a nucleus? What are the unique properties of short-lived nuclei having extreme values of N/Z ? What are the properties of effective nuclear interactions in the environment different from that in stable nuclei? There is also an unsettled question of what can be the largest possible atomic number Z of an atomic nucleus. The recent experiments in Dubna claim the existence of a $Z = 114, 115, 116, 117, 118$ system [1–11], with confirmation of hot fusion cross-sections coming from GSI [12] and LBL Berkeley [13]. For lighter elements: $Z = 107, 108, 109, 110, 111, 112$ successful syntheses were done at the GSI laboratory [14–23].

The presented tables contain ground state (g.s.) and saddle point (s.p.) properties of even-even superheavy nuclei that were obtained within the microscopic-macroscopic method in a multidimensional deformation space. This conceptually

simple method is very convenient for determining many nuclear properties with relatively high accuracy, unattainable by other models, particularly in the area of heaviest elements. It makes possible global calculations of fission properties in this area of the atomic nuclei. Such systematic predictions relate to the questions specified above and contribute to a view on this exotic nuclear domain. At the same time, they can help in the interpretation of present experiments and inspire efforts towards new ones.

Atomic masses (binding energies) have been experimentally determined for nearly 2300 nuclei [24]. For almost 800 nuclei mass is measured more precisely than to 5 keV, for other 1000 nuclei - with the accuracy of 5-50 keV. The binding energy determines energy available for nuclear reactions and decays (and thus the creation of elements by stellar nucleosynthesis), and holds the key to the fundamental question of how the heavy elements came to existence. The best available theoretical global mass calculations predict the mass values with an approximate deviation 500-800 keV. Ground state masses calculated within the Hartree-Fock-Bogoliubov (HFB) method [25, 26] fitted to the fission data through adjustment of a vibrational term in the phenomenological collective correction have the r.m.s deviation equal 0.729 MeV. Macroscopic-microscopic global calculations of nuclear ground state masses made by P. Moller and co-workers [27] give the r.m.s error 0.669 MeV for nuclei ranging from Oxygen to Hassium and 0.448 MeV in the case of nuclei above $N = 65$. Phenomenological formula with the 10 free parameters given by Duflo and Zuker [28, 29] gives mass estimates with the 0.574 MeV r.m.s error. So, nuclear masses are presently measured at least ten times more precisely than they can be calculated.

Although theoretical predictions sometimes differ quantitatively, they consistently predict prolate deformed super-heavy nuclei with $Z = 100-112$, which is confirmed experimentally for nuclei around ^{254}No [30], and spherical or oblate deformed systems with $Z = 114$ and $N = 174-184$ [31–36]. There are relatively many published predictions of the ground state properties of heaviest elements [25–29, 37]. Much rarer are analogous calculations at the saddle points, although they are necessary to estimate the cross sections (survival probabilities) for the synthesis of SHN [38]. This work provides the necessary theoretical saddle point data.

As the principle of the macroscopic -microscopic method is well known, only a brief description of it is given in Sect. 2, specifying involved quantities, their computation and the adopted values of parameters. In Sect. 3 we describe a variety of considered nuclear shapes which is an important ingredient of the model. The method for saddle point search is described in section 4, numerical tests applied to certify the results are mentioned in Sect. 5. Results and discussion are given in Sect. 6, a short summary in Sect. 7.

2. Method

The total nuclear binding energy (E), which depends on the proton number Z , and neutron number N and the nuclear shape, can be written as a sum of a macroscopic (E_{mac}) and a microscopic (E_{mic}) energy:

$$E(def, Z, N) = E_{mic}(def, Z, N) + E_{mac}(def, Z, N). \quad (1)$$

2.1. Macroscopic energy

The macroscopic part of atomic mass is a sum of masses of atomic constituents and the macroscopic energy. As E_{mac} , it is a smooth function of proton and neutron number. In our analysis, it is taken in the liquid-drop form [41, 42]:

$$\begin{aligned}
M_{\text{macr}}(Z, N, \beta_\lambda^0) &= M_{\text{H}}Z + M_{\text{n}}N - a_{\text{v}}(1 - \kappa_{\text{v}}I^2)A + a_{\text{s}}(1 - \kappa_{\text{s}}I^2)A^{2/3}B_{\text{S}}(\{\beta_\lambda^0\}) \\
&+ a_0A^0 + c_1Z^2A^{-1/3}B_{\text{C}}(\{\beta_\lambda^0\}) - c_4Z^{4/3}A^{-1/3} \\
&+ f(k_{\text{F}}r_{\text{p}})Z^2A^{-1} - c_{\text{a}}(N - Z) - a_{\text{el}}Z^{2.39},
\end{aligned} \tag{2}$$

where M_{H} is mass of the hydrogen atom, M_{n} is mass of neutron, $I = (N - Z)/A$ is the relative neutron excess, $A = Z + N$ is the mass number of a nucleus. The functions $B_{\text{S}}(\beta_\lambda)$ and $B_{\text{C}}(\beta_\lambda)$ describe the dependence of the surface and Coulomb energies, respectively, on deformations β_λ , and β_λ^0 are the values of these deformations at equilibrium. We adopted these functions in the form given by the Yukawa-plus-exponential model formulated by Krappe and Nix [41]. They read [27, 43]:

$$B_{\text{S}} = \frac{A^{-2/3}}{8\pi^2 r_0^2 a^4} \int \int_V \left(2 - \frac{r_{12}}{a}\right) \frac{e^{-r_{12}/a}}{r_{12}/a} d^3 r_1 d^3 r_2, \tag{3}$$

$$B_{\text{C}} = \frac{15}{32\pi^2} \frac{A^{-5/3}}{r_0^5} \int \int_V \frac{1}{r_{12}} \left[1 - \left(1 + \frac{1}{2} \frac{r_{12}}{a_{\text{den}}}\right) e^{-r_{12}/a_{\text{den}}}\right] d^3 r_1 d^3 r_2, \tag{4}$$

where $r_{12} = |\vec{r}_1 - \vec{r}_2|$ with \vec{r}_1 and \vec{r}_2 describing the positions of two interacting volume elements, a is the range of the Yukawa interaction on which the model is based, a_{den} is the range of the Yukawa function used to generate nuclear charge distribution. The functions are normalized in such a way that they are equal 1 for a spherical nucleus in the limit case of $a=0$ (for B_{S}) and $a_{\text{den}}=0$ (for B_{C}), corresponding to the traditional liquid-drop model with a sharp surface. The integrations are over the volume of a nucleus. After turning them into surface integrals, B_{S} and B_{C} were calculated by using a four-fold (or three-fold, for axial symmetry) 64-point Gaussian quadrature.

The quantities c_1 and c_4 appearing in the Coulomb energy and the Coulomb exchange correction, respectively, are

$$c_1 = \frac{3}{5} \frac{e^2}{r_0}, \quad c_4 = \frac{5}{4} \left(\frac{3}{2\pi}\right)^{2/3} c_1, \tag{5}$$

where e is the elementary electric charge and r_0 is the nuclear-radius parameter. The quantity $f(k_{\text{F}}r_{\text{p}})$ appearing in the proton form-factor correction to the Coulomb energy in Eq. (2) has the form

$$f(k_{\text{F}}r_{\text{p}}) = -\frac{1}{8} \frac{e^2 r_{\text{p}}^2}{r_0^3} \left[\frac{145}{48} - \frac{327}{2880} (k_{\text{F}}r_{\text{p}})^2 + \frac{1527}{1209600} (k_{\text{F}}r_{\text{p}})^4 \right], \tag{6}$$

where the Fermi wave number is

$$k_{\text{F}} = \left(\frac{9\pi Z}{4A}\right)^{1/3} r_0^{-1}, \tag{7}$$

and r_{p} is the proton root-mean-square radius. The last term in Eq. (2) describes the binding energy of electrons and a_{v} , κ_{v} , a_{s} , κ_{s} , a_0 , c_{a} are adjustable parameters. Thus, only two of these parameters (a_{s} and κ_{s}) appear at the term, which depends on deformation. The four remaining parameters stand at the terms independent of the shape of a nucleus.

The macroscopic part of mass, Eq. (2), is used the same as in [42], except that three of its adjustable parameters: a_{v} , κ_{v} and a_0 were fitted to experimental masses of even-even heaviest nuclei with $Z \geq 84$. The result was

$$a_{\text{v}} = 16.0643, \quad \kappa_{\text{v}} = 1.9261, \quad a_0 = 17.926. \tag{8}$$

Following the authors of [42], we omit here the two terms considered in [43]: charge-asymmetry term $c_{\text{a}}(N - Z)$ and Wigner term (characterized by a coefficient W), as they do not significantly change the quality of the description of

masses of heaviest nuclei. The values of other parameters are adopted after [43]:

$$a_s = 21.13 \text{ MeV}, \quad \kappa_s = 2.30, \quad (9)$$

$$\begin{aligned} a &= 0.68 \text{ fm}, & a_{\text{den}} &= 0.70 \text{ fm}, & r_0 &= 1.16 \text{ fm}, \\ r_p &= 0.80 \text{ fm}, & a_{\text{el}} &= 1.433 \cdot 10^{-5} \text{ MeV}. \end{aligned} \quad (10)$$

2.2. Microscopic energy

The Strutinski shell correction [44, 45], based on the deformed Woods-Saxon single-particle potential, is taken for the microscopic part:

$$\begin{aligned} E_{\text{mic}}(\text{def}, Z, N) &= E_{\text{corr}}^{\text{sh}}(\text{def}, Z, N) \\ &+ E_{\text{corr}}^{\text{pair}}(\text{def}, Z, N), \end{aligned} \quad (11)$$

where $E_{\text{corr}}^{\text{sh}}$ and $E_{\text{corr}}^{\text{pair}}$ are the shell and pairing corrections, respectively.

2.2.1. Woods-Saxon potential

The Woods-Saxon potential V_{WS} has the following form:

$$V_{\text{WS}}(\vec{r}) = -\frac{V}{1 + e^{d(\vec{r}, \text{def})/a_{\text{ws}}}}, \quad (12)$$

where V is the depth of the potential, $d(\vec{r}, \text{def})$ is the distance from the point \vec{r} to the surface of the nucleus, a_{ws} is the diffuseness of the nuclear surface. The symbol *def* stands for deformation which defines the nuclear surface (see Sect. 3). The depth of the potential is

$$V = V_0(1 \pm \kappa I), \quad (13)$$

where $I = (N - Z)/A$ is the relative neutron excess and V_0 and κ are adjustable parameters. The sign (+) is for protons and (−) for neutrons.

In the case of spherical shape, the potential is

$$V_{\text{WS}}(\vec{r}) = -\frac{V}{1 + e^{(r-R_0)/a_{\text{ws}}}}, \quad (14)$$

where $R_0 = r_0 A^{1/3}$.

The full microscopic potential has the form (e.g. [47]):

$$V_{\text{micr}} = V_{\text{WS}} + \lambda \left(\frac{\hbar}{2mc} \right)^2 \left(\frac{A}{A-1} \right)^2 (\nabla V_{\text{WS}}^{\text{s.o.}}) \cdot (\vec{\sigma} \times \vec{p}/\hbar) + V_c, \quad (15)$$

where the second term is the spin-orbit potential and the third term is the Coulomb potential, which has the following form:

$$V_c(\vec{r}) = \rho_c \int \frac{d^3 r'}{|\vec{r} - \vec{r}'|}, \quad (16)$$

where $\rho_c = 3(Z-1)e/(4\pi R_0^3)$ is the uniform density and the integration extends over the volume enclosed by the nuclear surface.

Here we use the "universal" set of parameters of the potential given in [47]

$$\begin{aligned} r_0 &= 1.275 \text{ fm}, & (r_0)_{\text{so}} &= 1.32 \text{ fm}, & \lambda &= 36.0 \text{ for protons,} \\ r_0 &= 1.347 \text{ fm}, & (r_0)_{\text{so}} &= 1.31 \text{ fm}, & \lambda &= 35.0 \text{ for neutrons,} \\ V_0 &= 49.6 \text{ MeV}, & a_{\text{ws}} &= 0.70 \text{ fm}, & \kappa &= 0.86, \end{aligned}$$

where r_0 and $(r_0)_{\text{so}}$ are the radius parameters for the central and spin-orbit parts of the potential, respectively.

The single-particle potential is diagonalized in the deformed-oscillator basis. The $n_p = 450$ lowest proton levels and $n_n = 550$ lowest neutron levels from the $N_{\text{max}} = 19$ lowest shells of the deformed harmonic oscillator are taken into account in the diagonalization procedure. We have determined the single - particle spectra for every investigated nucleus. These calculations therefore do not include any scaling relation to the *central* nucleus. A standard value of $\hbar\omega_0 = 41/A^{1/3}$ MeV is taken for the oscillator energy.

2.2.2. Shell correction

The shell correction energy is calculated as proposed by Strutinski [44, 45]:

$$E_{\text{corr}}^{\text{sh}} = E_{\text{micro}} - \tilde{E}_{\text{micro}}, \quad (17)$$

where E_{micro} is the sum of single-particle energies over all occupied energy levels,

$$E_{\text{micro}} = \sum_{\nu_{\text{occ}}} \varepsilon_{\nu} = \int_{-\infty}^{\varepsilon_{\text{F}}} \rho(\varepsilon) \varepsilon d\varepsilon, \quad (18)$$

and

$$\rho(\varepsilon) = \sum_{\nu} \delta(\varepsilon - \varepsilon_{\nu}) \quad (19)$$

is the density of the single-particle levels per energy unit, ε_{F} is the Fermi energy and ε_{ν} is the energy of a single-particle level ν .

The "smooth" microscopic energy \tilde{E}_{micro} is defined by means of the "smooth" density of the single-particle levels $\tilde{\rho}(\varepsilon)$:

$$\tilde{E}_{\text{micro}} = \int_{-\infty}^{\tilde{\varepsilon}_{\text{F}}} \tilde{\rho}(\varepsilon) \varepsilon d\varepsilon. \quad (20)$$

The value of $\tilde{\varepsilon}_{\text{F}}$, found from the following condition for the particle number N :

$$N = \int_{-\infty}^{\varepsilon_{\text{F}}} \rho(\varepsilon) d\varepsilon = \int_{-\infty}^{\tilde{\varepsilon}_{\text{F}}} \tilde{\rho}(\varepsilon) d\varepsilon, \quad (21)$$

is in general different from the Fermi energy ε_{F} .

The "smooth" density, appearing in (20) and (21), is obtained as

$$\tilde{\rho}(\varepsilon) = \frac{1}{\gamma} \int_{-\infty}^{\infty} \rho(\varepsilon') f_p \left(\frac{\varepsilon' - \varepsilon}{\gamma} \right) d\varepsilon', \quad (22)$$

where f_p is a folding function of the Gaussian type, taken as the formal expansion of the δ -function, truncated to the first $2p$ terms:

$$f_p(x) = \frac{1}{\sqrt{\pi}} \sum_{n=0}^{2p} C_n H_n(x) e^{-x^2}, \quad (23)$$

with

$$C_n = \frac{1}{2^n n!} H_n(0) = \begin{cases} \frac{(-1)^{\frac{n}{2}}}{2^n (\frac{n}{2})!} & \text{for even } n \\ 0 & \text{for odd } n. \end{cases} \quad (24)$$

The width γ is of the order of shell energy gaps. Using f_p one obtains the averaged density $\tilde{\rho}$:

$$\tilde{\rho}(\varepsilon) = \frac{1}{\gamma\sqrt{\pi}} \sum_{\nu=1} e^{-u_\nu^2} \sum_{n=0}^{2p} C_n H_n(u_\nu), \quad (25)$$

where $u_\nu = (\varepsilon - \varepsilon_\nu)/\gamma$.

The energy (20) in general depends on the parameters γ and p . The method is meaningful, if there is a certain interval of γ and corresponding p , for which the energy does not practically depend on them (so called "plateau condition"). Here, we use $\gamma = 1.2\hbar\omega_0$ for the Strutinski smearing parameter and a sixth-order correction polynomial for f_p .

2.2.3. Pairing correlations

In this work, pairing is included within the Bardeen-Cooper-Schrieffer (BCS) theory [48]. We assume a constant matrix element G of the (short-range) monopole pairing interaction. The hamiltonian of a system of nucleons, separately for neutrons and protons, may be written as:

$$H = \sum_{\nu} \varepsilon_{\nu} a_{\nu}^{\dagger} a_{\nu} - G \sum_{\nu, \nu' > 0} a_{\nu}^{\dagger} a_{\nu'}^{\dagger} a_{\nu'} a_{\nu}, \quad (26)$$

where ε_{ν} denotes the energy of a single-particle state ν . Each state ν has its time-reversal-conjugate $\bar{\nu}$ with the same energy (Kramers degeneration).

As the BCS wave function is a superposition of components with different numbers of particles, one requires that the expectation value of the particle number has a definite value N :

$$\langle \hat{N} \rangle = 2 \sum_{\nu > 0} v_{\nu}^2 = N. \quad (27)$$

The occupation numbers are given by

$$v_{\nu}^2 = \frac{1}{2} [1 - (\varepsilon_{\nu} - \lambda)/E_{\nu}], \quad (28)$$

where

$$E_{\nu} = \sqrt{(\varepsilon_{\nu} - \lambda)^2 + \Delta^2}. \quad (29)$$

The parameters λ and Δ are solutions of the system of two equations, for the average particle number and the pairing gap:

$$N = \sum_{\nu > 0} \left[1 - \frac{\varepsilon_{\nu} - \lambda}{\sqrt{(\varepsilon_{\nu} - \lambda)^2 + \Delta^2}} \right] \quad (30)$$

$$\frac{2}{G} = \sum_{\nu > 0} \frac{1}{\sqrt{(\varepsilon_{\nu} - \lambda)^2 + \Delta^2}}. \quad (31)$$

For the energy of the system in the BCS state, one gets:

$$E_{\text{BCS}} = 2 \sum_{\nu > 0} \varepsilon_{\nu} v_{\nu}^2 - \frac{\Delta^2}{G} - G \sum_{\nu > 0} v_{\nu}^4. \quad (32)$$

2.2.4. Pairing correction

Pairing correction energy $E_{\text{corr}}^{\text{pair}}$ is usually constructed in analogy to the shell correction energy $E_{\text{corr}}^{\text{sh}}$,

$$E_{\text{corr}}^{\text{pair}} = E_{\text{pair}} - \tilde{E}_{\text{pair}}, \quad (33)$$

where E_{pair} is the pairing energy corresponding to real single-particle level distribution $\rho(\varepsilon)$, Eq. (19), and \tilde{E}_{pair} is this energy for the smoothed s.p. level distribution, $\tilde{\rho}(\varepsilon)$, Eq. (22).

The E_{pair} is

$$E_{\text{pair}} = E_{\text{BCS}} - E_{\text{BCS}}^{\Delta=0}, \quad (34)$$

where $E_{\text{BCS}}^{\Delta=0}$ is the E_{BCS} energy in the limit of disappearing pairing correlations ($\Delta = 0$). Thus, using Eq. (32),

$$E_{\text{BCS}}^{\Delta=0} = 2 \sum_{\nu=1}^{N/2} \varepsilon_{\nu} - \frac{GN}{2}. \quad (35)$$

because for $\Delta = 0$, the probability v_{ν}^2 of the occupation of any state ν is either 0 or 1.

The smoothed pairing energy term is included in a schematic form, resulting from a model with a constant level density of pairs (doubly degenerate levels) $\bar{\rho}$, taken equal to $\tilde{\rho}(\tilde{\varepsilon}_{\text{F}})/2$

$$\tilde{E}_{\text{pair}} = -\frac{N_p^2}{\bar{\rho}}(\sqrt{1+x^2}-1) + \frac{\bar{G}N_p x}{2} \arctan(1/x). \quad (36)$$

In the above expression, $x = \bar{\rho}\bar{\Delta}/N_p$, $N_p = N/2$ is a number of pairs, $\bar{\Delta}$ is an average value of the pairing gap in the neighbourhood of a studied nucleus, related to the average pairing strength \bar{G} via the BCS formula for a constant level density

$$\frac{1}{\bar{G}\bar{\rho}} = \ln \left(\frac{\sqrt{1+x^2}+1}{x} \right). \quad (37)$$

The values of $\bar{\Delta}$ are taken from the fit [46]

$$\bar{\Delta} = \frac{5.72}{N^{1/3}} \exp(-0.119I - 7.89I^2) \quad (38)$$

for neutrons and

$$\bar{\Delta} = \frac{5.72}{Z^{1/3}} \exp(0.119I - 7.89I^2), \quad (39)$$

for protons, with $I = (N - Z)/A$. The smoothed pairing energy term calculated in this way shows nearly no deformation dependence, for example, it varies by about 50 keV over the whole deformation range in actinides. Thus, it could be omitted in energy landscapes, while it shows up in binding energies.

The pairing interaction strengths G , Eq. (26), are taken as

$$G_l = (g_{0l} + g_{1l}I)/A, \quad (40)$$

where the index l stands for p (protons) or n (neutrons).

The strengths G_l were fixed by adjusting the gap parameter Δ to the three-point odd-even mass differences

$$\Delta_Z M = (-1)^Z \left\{ \frac{1}{2} [M(Z+1, N) + M(Z-1, N)] - M(Z, N) \right\},$$

$$\Delta_N M = (-1)^N \left\{ \frac{1}{2} [M(Z, N+1) + M(Z, N-1)] - M(Z, N) \right\}.$$

The adjustment, using all measured masses of nuclei with $Z \geq 88$, resulted in the values [42]:

$$\begin{aligned} g_{0l} &= 17.67 \text{ MeV}, & g_{1l} &= -13.11 \text{ MeV}, & \text{for } l = n \text{ (neutrons)}, \\ g_{0l} &= 13.40 \text{ MeV}, & g_{1l} &= 44.89 \text{ MeV}, & \text{for } l = p \text{ (protons)}. \end{aligned} \quad (41)$$

3. Shape parametrization

The essential point of any microscopic-macroscopic study is the kind and dimension of the deformation space used to describe a variety of nuclear shapes. This is particularly important for finding the saddle point along a fission path. Of course, there is no ideal shape parametrization. As far as we are interested in superheavy nuclei, with comparatively short fission barriers, a traditional expansion of the nuclear radius in spherical harmonics [49], can be used. We admit shapes of a 10D manifold defined by:

$$\begin{aligned} R(\vartheta, \varphi) = R_0 c(\{\beta\}) \{ & 1 + \beta \left[\cos \gamma Y_{20} + \sin \gamma Y_{22}^{(+)} \right] \\ & + \beta_{40} Y_{40} + \beta_{42} Y_{42}^{(+)} + \beta_{44} Y_{44}^{(+)} \\ & + \beta_{30} Y_{30} + \beta_{50} Y_{50} + \beta_{70} Y_{70} \\ & + \beta_{60} Y_{60} + \beta_{80} Y_{80} \}. \end{aligned} \quad (42)$$

The real spherical harmonics $Y_{lm}^{(+)}$ are defined as:

$$Y_{lm}^{(+)} = \frac{1}{\sqrt{2}} [Y_{lm} + (-1)^m Y_{l-m}], \quad \text{for } m \neq 0. \quad (43)$$

We use the conventional notation:

$$\begin{aligned} \beta_{20} &= \beta \cos \gamma, \\ \beta_{22} &= \beta \sin \gamma, \end{aligned} \quad (44)$$

where γ is the Bohr quadrupole non-axiality parameter. The function $c(\{\beta\})$ is determined by the volume-conservation condition.

There is no physical principle which would forbid nonaxial ground-state nuclear shapes. However, calculations by Möller et al. [50] and our studies [51–53] suggest that in the investigated nuclei the effect of nonaxiality (including octupole Y_{32}^+) in ground states is either small or non-existent. On the other hand, competing axially symmetric minima are frequent [54]. Therefore, we assumed here the axial symmetry of the ground states. The energy is minimized simultaneously in all axial degrees of freedom: $\beta_{20}, \beta_{30}, \beta_{40}, \beta_{50}, \beta_{60}, \beta_{70}, \beta_{80}$, using a multidimensional conjugate gradient method.

The saddle point is defined as a *minimum* over all paths connecting the ground state with the behind-the barrier region of the *maximal* energies along each path. Practical calculations are performed as follows. Energy is calculated at the following grid points (with steps given in parentheses):

$$\begin{aligned} \beta \cos \gamma &= 0(0.05)0.65, \\ \beta \sin \gamma &= 0(0.05)0.40, \\ \beta_{40} &= -0.20(0.05)0.20. \end{aligned} \quad (45)$$

Then, energy is interpolated (by the standard SPLIN3 procedure of the IMSL library) on the grid five times denser in each direction. Thus, we finally have energy values at a total of 110946 grid points. In order to find the saddle point a two-step method is used. First, on such a 3-dimensional grid $(\beta_{20}, \beta_{22}, \beta_{40})$, the saddle point is determined by the Dynamic Programming Method given in [55] and adopted to the fission process by Baran et al. [56]. Then, with these three deformations fixed, energy is minimized with respect to the other degrees of freedom: $\beta_{42}, \beta_{44}, \beta_{30}, \beta_{50}, \beta_{60}, \beta_{70}, \beta_{80}$. In the previous calculations [57, 58], the nonaxial hexadecapole deformations have usually been treated as functions of the quadrupole triaxiality angle γ . In the present calculations, the hexadecapole nonaxialities β_{42} and β_{44} are independent variables.

4. Dynamic programming method

It is always possible to convert an m -dimensional grid: $(n_1 \times n_2 \times n_3 \times \dots \times n_m)$ into a four dimensional grid: $(n_1 \times n_2 \times n_3 \times N)$, $N = n_4 \times n_5 \times n_6 \times \dots \times n_m$. In the case of our deformation space: n_1 refers to β_{20} (elongation), n_2 to γ (nonaxiality), n_3 to β_{40} (neck). The N - axis describes all other degrees of freedom which we use for the description of shapes (all other multipolarities). Each path i , connecting the starting point with a behind-the-barrier point $n + 1$, may be characterized by the maximal value of energy E_{max}^i which one can find along it, where i is the index of a given path. The energy values between two neighboring points on a given path are investigated with the help of an interpolation procedure. In this way, we have a set of all possible paths i , connecting the starting point to the $n + 1$ -th point, with the value of the maximal energy E_{max}^i on each. It is obvious that the saddle-point energy will be the minimal value of all E_{max}^i over all possible paths (all possible i). The trajectory corresponding to this minimal value will automatically pass through the saddle point. It appears that to find the right trajectory along which E_{max}^i is minimal we do not need to consider all possible trajectories.

5. Numerical tests and error checks

The important numerical tool exploited here is the minimization procedure. It is used to find the ground state energy in a 7-dimensional space and the saddle point energy by the 7-dimensional minimization. Multidimensional minimization is a mixed blessing method: from the one point of view, it gives us the opportunity to find minima in the large deformation spaces (infeasible on a grid) but from the other, it introduces the necessity to check whether or not, the obtained minima are indeed the global ones. In order to gain some confidence in our results we used a number of checks. The standard checks within the minimization routine include the monitoring of energy gradients. In addition, we looked at the continuity of the resulting deformation parameters with respect to $\beta \sin \gamma$ and $\beta \cos \gamma$ and at their stability with respect to the choice of their starting values. The starting values of the deformation parameters were always taken different from zero.

It should be also realized that we cannot be absolutely certain that the minimization in the second step of our saddle-point-search procedure does not lead to errors. The hope that the initial deformation net $(\beta \sin \gamma, \beta \cos \gamma, \beta_{40})$ may be sufficient is based mainly on the fact that other deformations are small and weakly coupled to those three. In addition, we have checked saddle point energies obtained in the first stage of our procedure on the 3D grid by comparing them to the results of the analogous procedure using the 2D $(\beta \sin \gamma, \beta \cos \gamma)$ and two variants of the 4D grids: $(\beta \sin \gamma, \beta \cos \gamma, \beta_{40}, \beta_{42})$

Table A

5D-IFW results

Z	N	E [MeV]	β_{20}^{sp}	β_{22}^{sp}	β_{40}^{sp}	β_{60}^{sp}	β_{80}^{sp}
108	166	-1.05	0.33	0.01	0.04	-0.01	0.05
112	174	-0.48	0.27	0.01	-0.04	0.04	0.02

and $(\beta \sin \gamma, \beta \cos \gamma, \beta_{40}, \beta_{44})$. An important test of the saddle-point searching method was the application of a completely different approach based on so-called "imaginary water flow" (IWF) [59–63]. This conceptually simple method is still numerically efficient in the 5-dimensional space of deformations $\beta \sin \gamma, \beta \cos \gamma, \beta_{40}, \beta_{60}, \beta_{80}$ and has been used for some nuclei. In order to avoid ambiguity, saddle points with vanishing parameters: β_{42}, β_{44} were chosen. The obtained results were practically identical with those of the previous method as one can see in Table A. One can see that the difference in barrier does not exceed 110 keV.

6. Discussion of the results

The calculated properties of ground-states of even-even nuclei are given in Table 1 and those of saddle-points in Table 2. Energy maps in $(\beta \cos \gamma, \beta \sin \gamma)$ plane, necessary to appreciate fission barriers, are shown in Fig. 1. They were obtained by minimization over 8 remaining deformations. Total energy shown in Tables and Figures is normalized in such a way that its macroscopic part is equal zero at the spherical shape.

6.1. Ground state properties

To find the ground state masses and shapes the total energy is minimized (using the gradient method) with respect to $\beta_{20}, \beta_{30}, \beta_{40}, \beta_{50}, \beta_{60}, \beta_{70}, \beta_{80}$. The candidates for the global minimum are chosen from the energy map (β_{20}, β_{22}) by inspection, taking into account barriers heights. Only in a few cases we obtained a small nonzero value of the octupole deformation and these are not given in Tables. Macroscopic and microscopic parts of total energy are shown in Fig. 3. The biggest shell effect (~ 9 MeV) is observed for ^{270}Hs ($Z = 108, N = 162$), the semi-magic nucleus. As in other Woods-Saxon micro-macro calculations, the second minimum (~ 7 MeV) of the shell correction is located around the nucleus $Z = 114$ and $N = 184$. When superposed with weakly deformation-dependent macroscopic part (Fig.3), this component is largely responsible for the emergence of global minima in superheavy nuclei.

6.1.1. Ground state shapes (deformations)

As mentioned in section 3, calculations including nonaxial shapes show that the ground states are usually axially symmetric. For $Z > 120$, there are a few minima exhibiting unusual shapes [54], but they are at most degenerate with the minima given in Table 1. In addition to typical prolate, spherical and oblate shapes, the superdeformed oblate (SDO) shapes with $\beta_{20} \approx -0.45$ appear for some $Z \approx 120$ nuclei, discussed in the recent work [65].

In the studied nuclei, up to $Z = 118$, the shape evolution starts with prolate shapes for small N and ends with oblate or spherical (close to $N = 184$) for largest N . The neutron-deficient $Z \geq 120$ nuclei have SDO ground states. With increasing N , they evolve into oblate, then spherical, then oblate again, but for $Z = 126$ all ground states are oblate. In some $Z \geq 120$ systems, SDO ground states reappear for largest N - see Fig. 1.

Table B

Statistical parameters of the calculated mass excess in relation to experimental or recommended atomic mass excess [64]. All quantities are in MeV, except for the number of nuclei N .

N	$\langle M_{gs}^{th} - M_{gs}^{exp} \rangle$	$Max M_{gs}^{th} - M_{gs}^{exp} $	r.m.s
67	0.43	1.58	0.58

Energy maps are necessary to study secondary minima and appreciate the competition of various shapes. The competition of prolate, spherical and oblate minima in $Z = 120$ nuclei may be seen in Fig. 1. Let us note that the apparent secondary prolate minima at $\beta_{20} \approx 0.4$ are so shallow that they cannot be seriously considered as candidates for equilibrium configurations. In neutron deficient isotopes, the prolate and SDO shapes compete. With increasing N , the prolate minimum disappears and normal oblate minimum becomes lower than the SDO minimum. The spherical configuration becomes the g.s. for $N = 180 - 184$. For still heavier isotopes (Table 1, not shown in Fig.1), the SDO minimum reappears as the g.s.

In Fig. 2, energy landscapes are shown for three experimental nuclei (one synthesized in GSI and two in Dubna) and one hypothetical $Z = 124$ system. The ^{276}Ds is prolate, the two heavier, $^{286}114$ and $^{294}118$, are weakly deformed and γ -soft, while $^{308}124$ is weakly oblate.

6.1.2. Ground state mass excess

The accuracy of the approach may be assessed by comparing calculated and experimental masses (ground state masses)[64]. The difference $M_{gs}^{th} - M_{gs}^{exp}$ is shown in Fig. 4 as a function of A and in Fig. 5 as a function of both Z and N . The accuracy is summarized in Table B below. The average discrepancy $\langle | M_{gs}^{th} - M_{gs}^{exp} | \rangle$, the maximal difference $Max | M_{gs}^{th} - M_{gs}^{exp} |$ and the *r.m.s.* deviation are shown for a number N of even-even superheavy nuclei.

The agreement between the calculated and experimental masses is the worst for nuclei located near $Z = 106$, $N = 162$ ($\simeq + 1.5$ MeV) and $Z = 114$, $N = 184$ ($\simeq -1.5$ MeV).

6.1.3. Q -alpha energies

Q_{α}^{th} values given in Table 2 are calculated always for g.s. to g.s transitions, even if the corresponding deformations differ widely and hence one can expect a substantial decay hindrance. Q_{α} energy for a nucleus with N neutrons and Z protons can be directly obtained from masses

$$Q_{\alpha}^{th}(Z, N) = M_{gs}^{th}(Z, N) - M_{gs}^{th}(Z - 2, N - 2) - M(2, 2). \quad (46)$$

The resulting discrepancies between calculated and experimental Q_{α} values are shown in Table C. The average discrepancy $\langle | Q_{\alpha}^{th} - Q_{\alpha}^{exp} | \rangle$, the maximal difference $Max | Q_{\alpha}^{th} - Q_{\alpha}^{exp} |$ and the *r.m.s.* deviation are shown for a number N of even-even superheavy nuclei.

The largest discrepancy between the calculated and experimental Q_{α} values results for nuclei located near $Z = 106$, $N = 162$, what is a consequence of the calculated masses in this area.

Table C

Statistical parameters of calculated Q_α energies in relation to experimental data [64]. All quantities are in MeV, except for the number of nuclei N.

N	$\langle Q_\alpha^{th} - Q_\alpha^{exp} \rangle$	$Max Q_\alpha^{th} - Q_\alpha^{exp} $	r.m.s
67	0.02	0.74	0.29

6.2. Saddle point properties

It is worth emphasizing that the saddles listed in Table 2 correspond to the ground states. In case that secondary minima exist, their saddle points may be *different* from that of the ground state. In other words, a saddle point always relates to a minimum (equilibrium, metastable state) whose decay it characterizes.

The used method of the search for saddles, the combined 3D saddle-point search and subsequent 7D minimization, implies that they may slightly differ from those read from the maps in $(\beta \cos \gamma, \beta \sin \gamma)$, shown in Figs. 2 and 3. The latter are fixed by the single 8D minimization for the purpose of illustration of an energy landscape. For example, the axially-symmetric saddle in $^{288}120$ seems to be lower than the triaxial one in Fig. 2, while it is the opposite in Table 2. The local shell correction and the macroscopic energy at the saddle point configuration has been shown in Fig. 9. Generally, we see that the shell effects at the saddle point are much weaker than in the ground state, but not negligible. The most pronounced effects (~ 3 MeV) were obtained around nuclei with $Z=102$, $N=162$ and $Z=114$, $N=184$. For the majority of nuclei, microscopic energy at the saddle point is negative while macroscopic energy is positive. Values of these energies are similar in magnitude.

6.2.1. Saddle point shapes (deformations)

The calculated saddles are mostly triaxial in $Z = 98 - 104$, and exclusively triaxial in $Z \geq 122$ nuclei. There are many triaxial saddles with rather sizable values of the deformation γ . Since the saddle deformation is a result of a competition between the axial and triaxial saddle energies, even their tiny difference may result in an abrupt change in γ^{sp} . This is reflected in the abrupt changes of γ^{sp} between neighbouring isotopes - Table 2. Stated otherwise, a large γ^{sp} does not necessarily correlate with a large nonaxiality effect on the saddle-point energy (mass).

6.2.2. Saddle point mass excess - fission barriers

Fission barriers may be obtained from Tables 1 and 2 as:

$$B_f = E_{sp}^{th} - E_{gs}^{th} = M_{sp}^{th} - M_{gs}^{th}. \quad (47)$$

Most of them were given and discussed in [66]. One can compare our barriers heights with other recent calculations [63, 67–70]. They are relevant for fission rates from excited states (thermal rates), with the excitation energy greater than, roughly, the barrier itself. The spontaneous fission rates involve an additional inertia effect, see e.g. [71].

7. Summary

Using the macroscopic-microscopic model, we have calculated the ground state and saddle point properties of even-even superheavy elements: masses, macroscopic energies, shell corrections, deformations as well as the ground state to

ground state alpha decay energies.

Acknowledgments

This work was supported by the Polish Ministry of Science and Higher Education, Contract No. JP201 0013570. One of the authors (P.J.) was co-financed by the European Social Fund and the state budget (within Sub-measure 8.2.2 Regional Innovation Strategies, Measure 8.2 Transfer of knowledge, Priority VIII Regional human resources for the economy Human Capital Operational Programme).

Table 1. Ground state properties

For the isotopes of the elements $Z=98-126$, tabulates the ground state masses, total energies, macroscopic and microscopic energies, equilibrium deformations and corresponding α -decay ground state to ground state Q -values.

Z	The atomic number
A	The mass number
M_{gs}^{th}	The mass excess in MeV
E	The total energy in MeV
E_{mac}	The macroscopic energy in MeV
E_{mic}	The microscopic energy in MeV
$\beta_{20}^{min} \div \beta_{80}^{min}$	The equilibrium deformations
Q_{α}	Theoretical Q -value in MeV

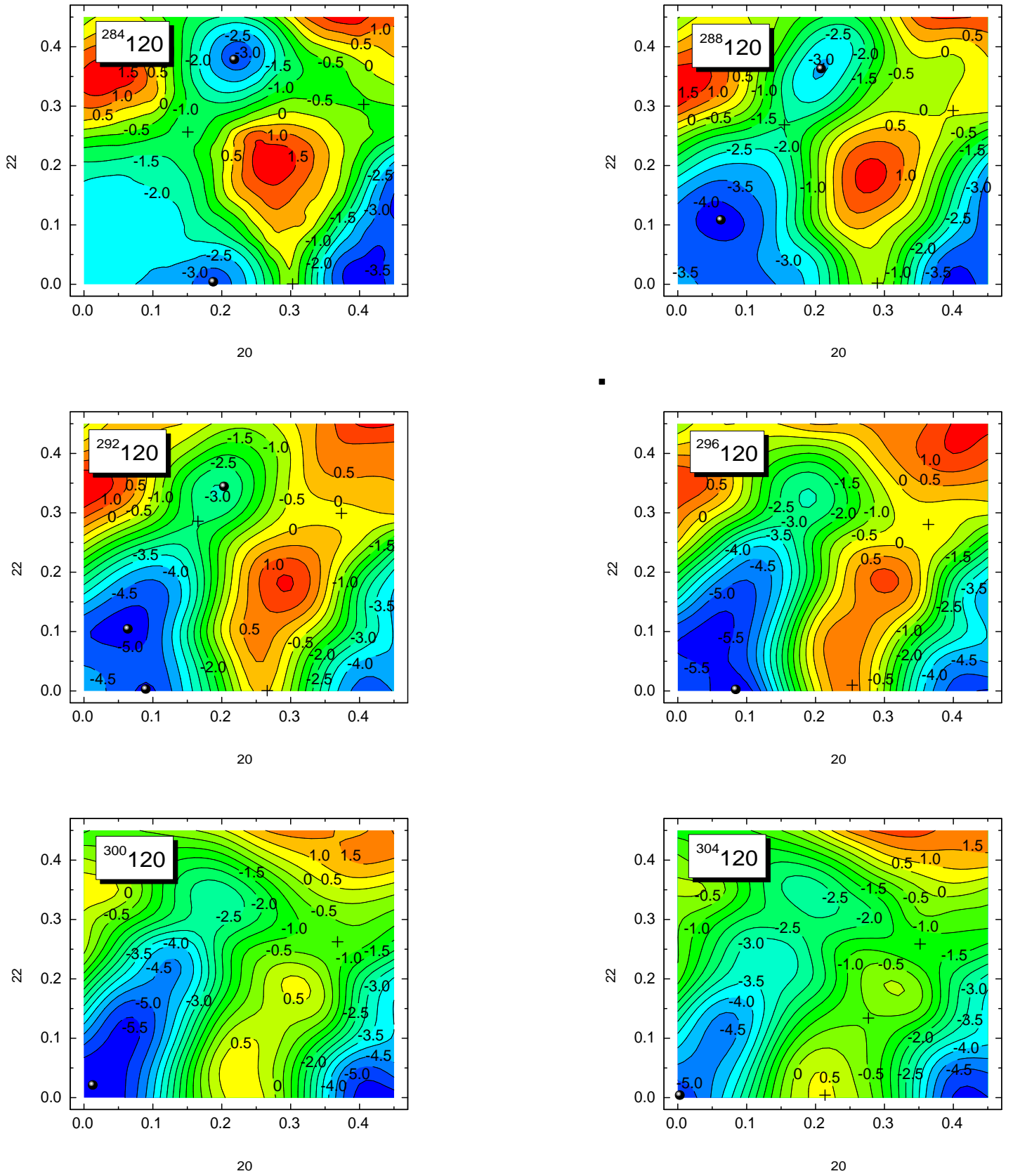


Fig. 1: Energy surfaces, $E - E_{mac}(sphere)$, for $Z = 120$ isotopes, resulting from the minimization over the remaining 8 deformations.

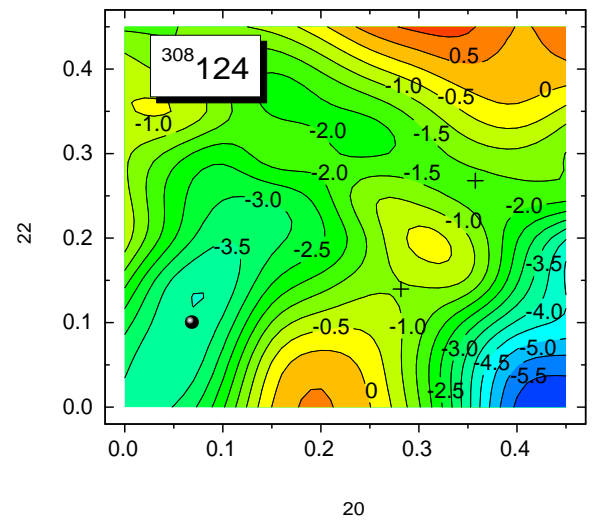
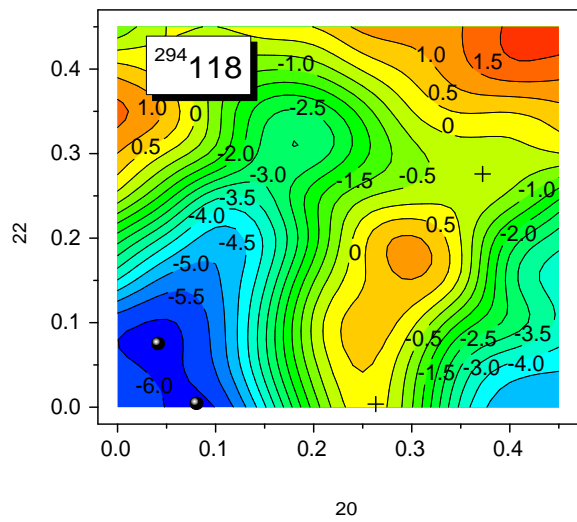
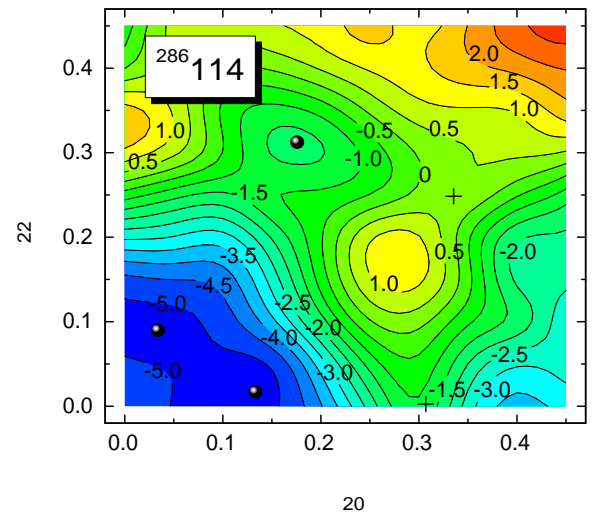
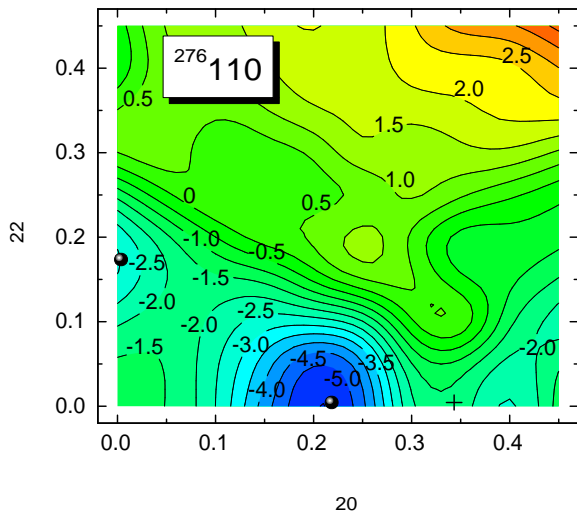


Fig. 2: As in Fig. 1, but for the three of experimentally detected evaporation residues and one hypothetical heavier system.

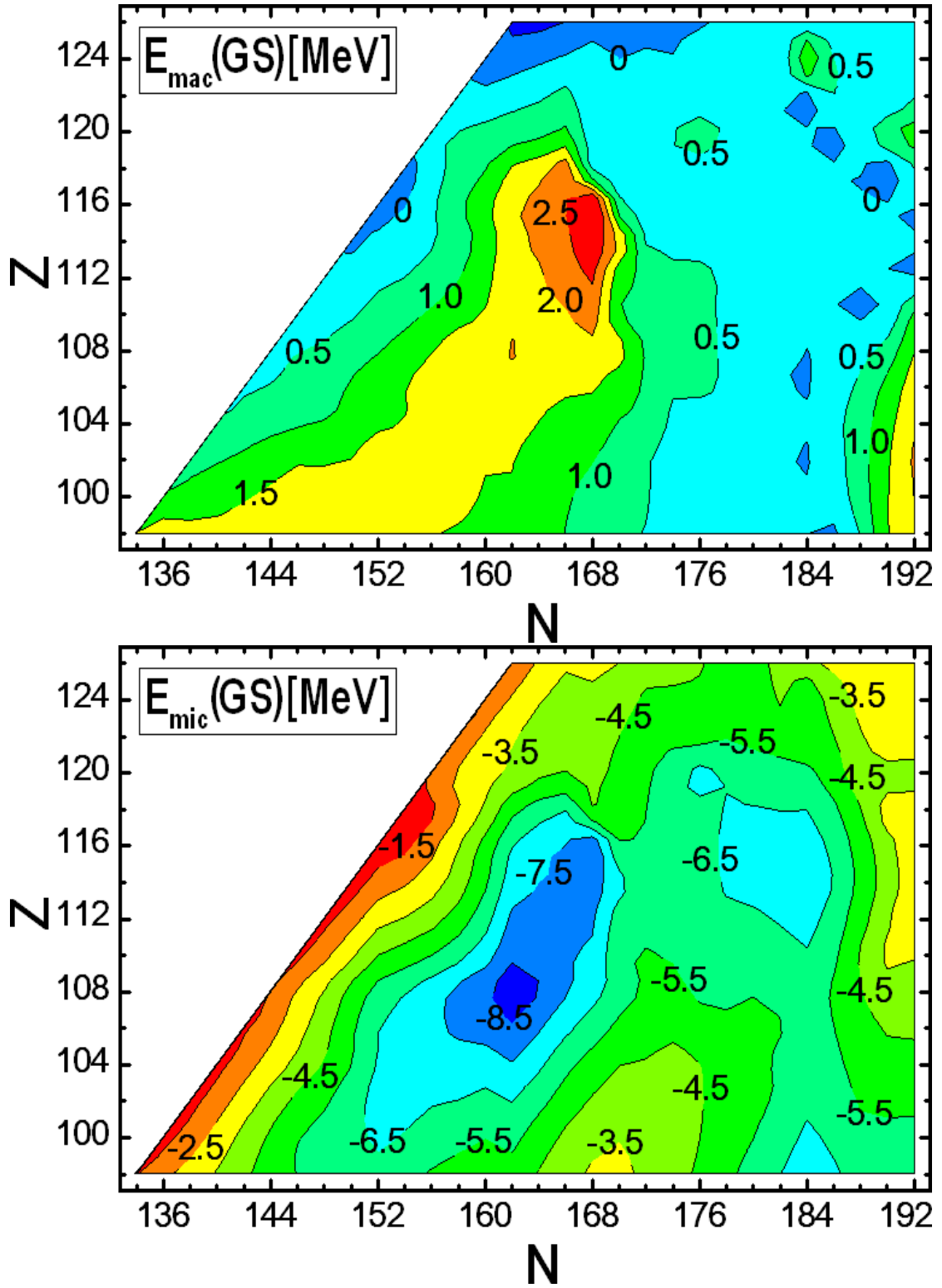


Fig. 3: Calculated macroscopic and microscopic components of the ground-state binding energy, $E_{\text{mac}} - E_{\text{mac}}(\text{sphere})$ and E_{micr} .

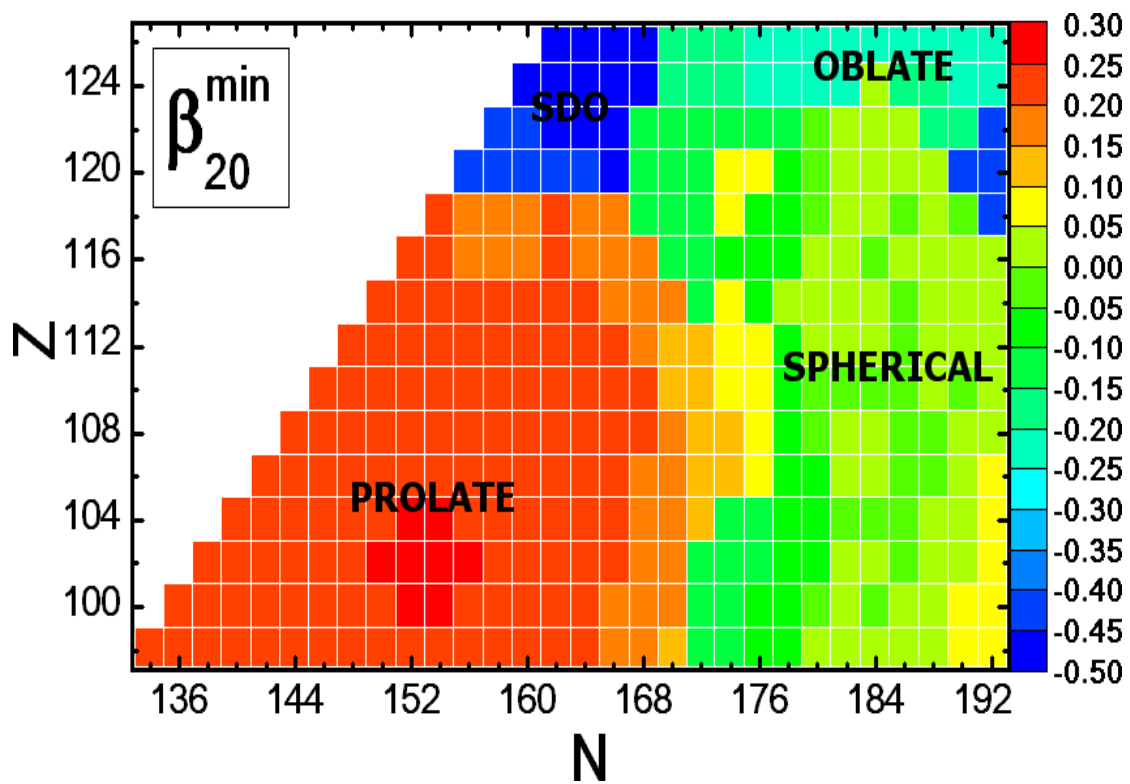


Fig. 4: Calculated ground-state quadrupole deformations.

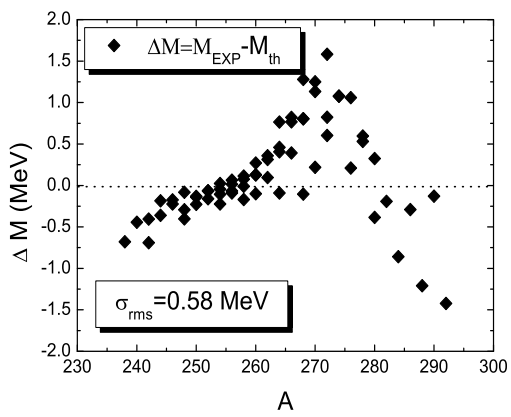


Fig. 5: Discrepancy between the measured and calculated nuclear masses vs mass number.

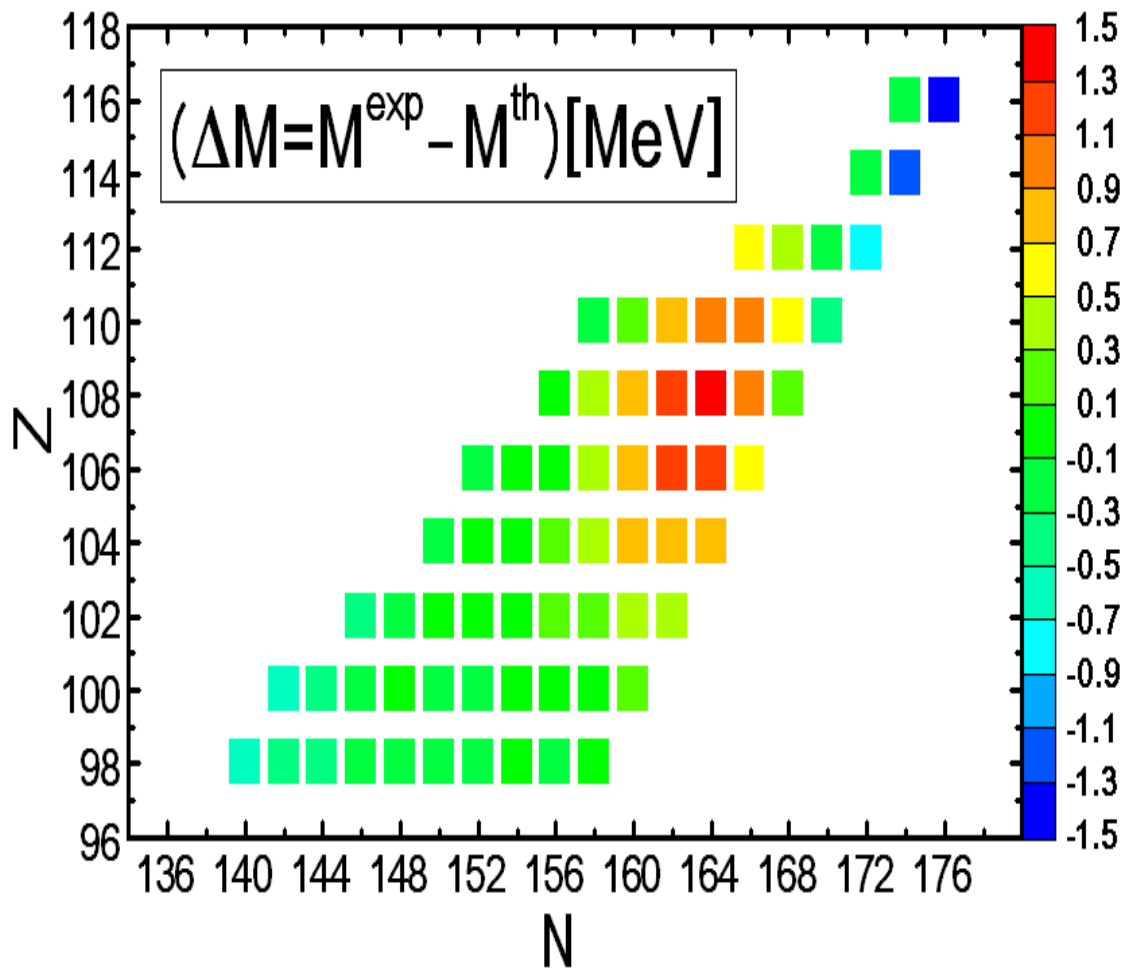


Fig. 6: As in Fig. 4, but as a function of proton and neutron numbers.

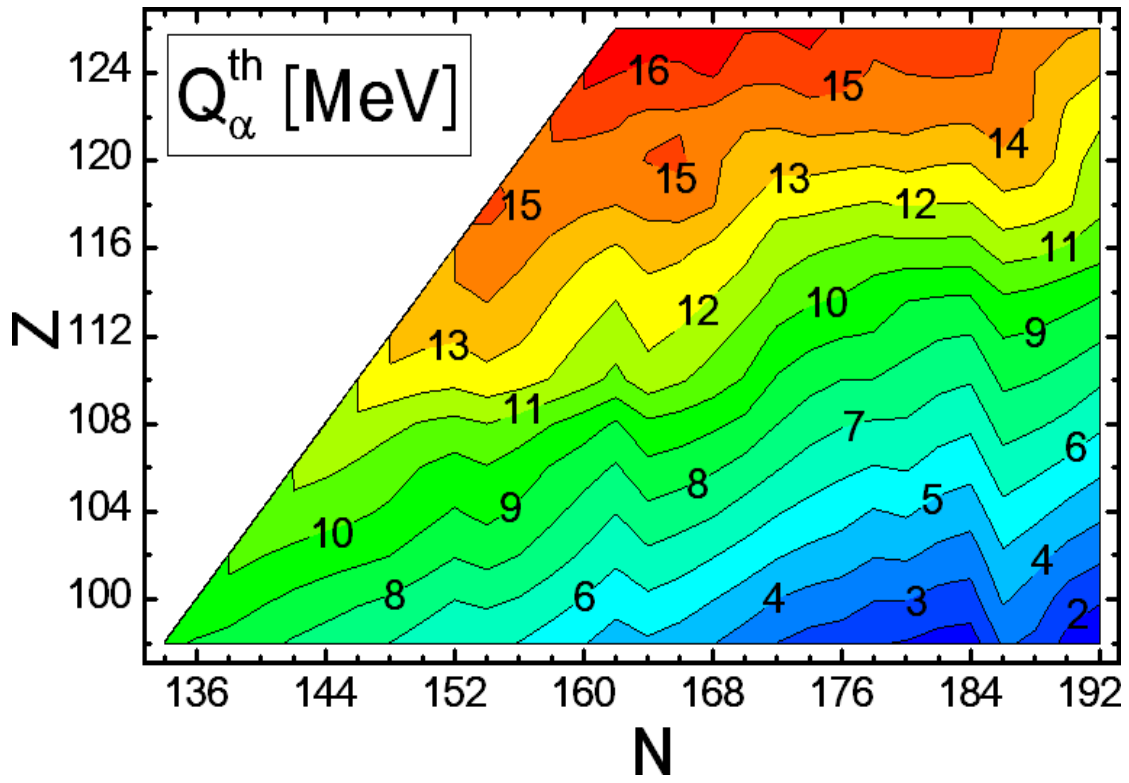


Fig. 7: Calculated α -decay energies for g.s. \rightarrow g.s transitions as a function of proton and neutron numbers.

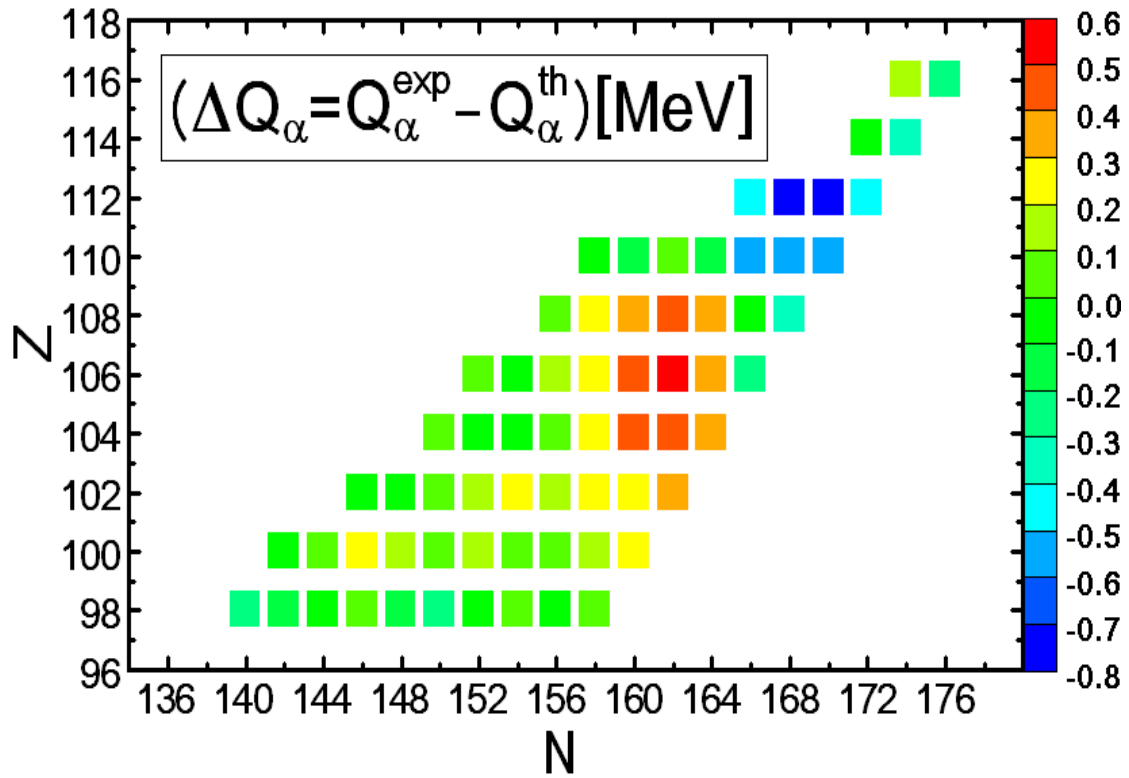


Fig. 8: Discrepancy between the experimental and calculated α -decay energies as a function of proton and neutron numbers.

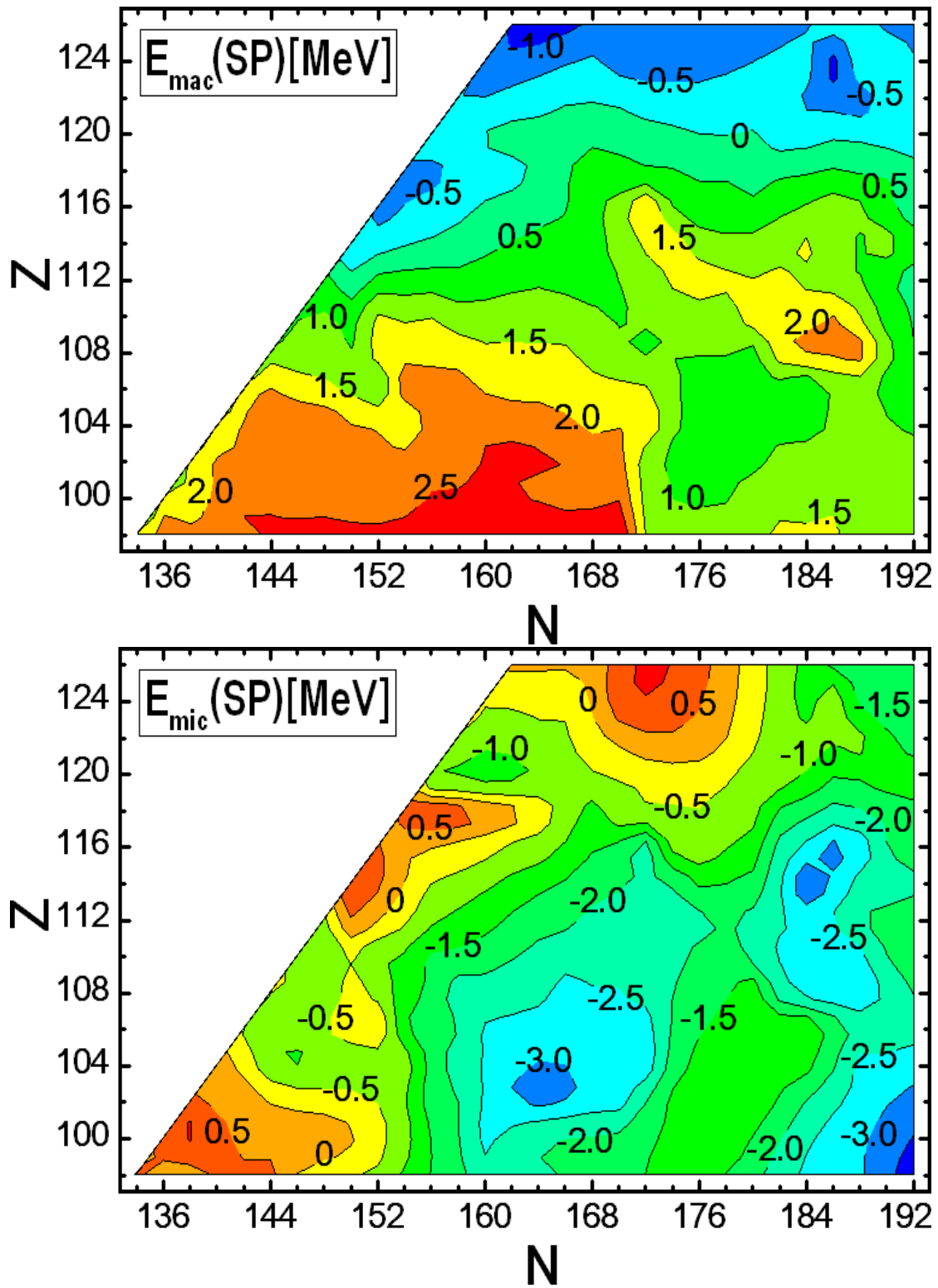


Fig. 9: As in Fig. 3, but for the calculated saddle points.

Table 1

Calculated Ground State Masses and Deformations.

Z	N	M_{gs}^{th}	E	E_{mac}	E_{mic}	β_{20}^{min}	β_{40}^{min}	β_{60}^{min}	β_{80}^{min}	Q_{alpha}
98	134	59.53	0.09	1.54	-1.46	0.210	0.081	0.009	-0.003	9.289
98	136	58.38	-0.61	1.68	-2.29	0.209	0.085	0.007	-0.004	8.883
98	138	57.86	-1.27	1.67	-2.95	0.214	0.084	0.001	-0.006	8.653
98	140	57.88	-1.99	1.66	-3.64	0.221	0.081	-0.007	-0.009	8.286
98	142	58.48	-2.69	1.68	-4.37	0.226	0.078	-0.014	-0.011	7.883
98	144	59.74	-3.28	1.73	-5.01	0.234	0.073	-0.023	-0.015	7.567
98	146	61.66	-3.77	1.82	-5.58	0.240	0.067	-0.030	-0.017	7.232
98	148	64.32	-4.05	1.67	-5.72	0.242	0.056	-0.035	-0.012	6.987
98	150	67.53	-4.30	1.50	-5.80	0.242	0.043	-0.038	-0.005	6.574
98	152	71.30	-4.50	1.60	-6.10	0.247	0.029	-0.046	0.002	6.138
98	154	76.10	-4.18	1.56	-5.74	0.248	0.019	-0.046	0.008	6.215
98	156	81.45	-3.80	1.52	-5.32	0.244	0.008	-0.045	0.013	5.966
98	158	87.13	-3.57	1.42	-4.99	0.238	-0.004	-0.041	0.016	5.503
98	160	93.12	-3.49	1.35	-4.84	0.235	-0.021	-0.032	0.018	5.055
98	162	99.36	-3.64	1.46	-5.10	0.223	-0.042	-0.022	0.020	4.526
98	164	106.70	-3.12	1.12	-4.24	0.209	-0.039	-0.013	0.013	4.843
98	166	114.39	-2.70	0.94	-3.65	0.191	-0.040	-0.005	0.008	4.528
98	168	122.20	-2.60	0.71	-3.30	0.165	-0.035	-0.001	0.005	4.042
98	170	130.12	-2.81	0.51	-3.32	0.141	-0.029	0.001	0.003	3.532
98	172	138.08	-3.40	0.46	-3.86	-0.138	0.018	0.009	-0.006	2.988
98	174	146.37	-4.07	0.28	-4.35	-0.115	0.008	0.006	-0.003	2.621
98	176	155.15	-4.64	0.20	-4.84	-0.097	-0.003	0.007	0.001	2.480
98	178	164.18	-5.36	0.22	-5.58	-0.088	-0.010	0.010	0.004	2.069
98	180	173.71	-5.96	0.01	-5.97	0.003	0.000	0.000	0.000	1.928
98	182	183.40	-6.79	0.01	-6.80	0.000	0.001	0.000	0.000	1.647
98	184	193.60	-7.47	0.01	-7.48	0.000	0.000	0.000	0.000	1.509
98	186	206.10	-6.22	0.04	-6.25	0.000	0.000	0.000	0.000	3.152
98	188	218.92	-5.00	0.94	-5.93	0.028	0.013	0.002	-0.001	2.786
98	190	231.48	-4.40	1.81	-6.21	0.056	0.031	0.004	-0.003	1.669
98	192	244.29	-3.88	2.05	-5.94	0.066	0.032	0.001	-0.003	1.005
100	136	71.84	-0.06	1.11	-1.17	0.231	0.065	-0.009	-0.006	9.885
100	138	70.38	-0.80	1.21	-2.02	0.232	0.066	-0.015	-0.007	9.567
100	140	69.44	-1.60	1.32	-2.92	0.233	0.066	-0.020	-0.009	9.156
100	142	69.09	-2.40	1.47	-3.87	0.236	0.066	-0.026	-0.011	8.784
100	144	69.37	-3.13	1.60	-4.73	0.240	0.062	-0.033	-0.014	8.467
100	146	70.31	-3.76	1.75	-5.51	0.245	0.057	-0.040	-0.015	8.146
100	148	71.99	-4.19	1.66	-5.85	0.247	0.047	-0.044	-0.009	7.900
100	150	74.22	-4.61	1.60	-6.20	0.248	0.034	-0.048	-0.002	7.474
100	152	76.98	-5.00	1.72	-6.72	0.251	0.023	-0.053	0.004	7.020
100	154	80.95	-4.70	1.66	-6.36	0.250	0.013	-0.052	0.009	7.222
100	156	85.47	-4.35	1.67	-6.01	0.248	0.001	-0.051	0.016	6.945
100	158	90.35	-4.12	1.64	-5.76	0.245	-0.012	-0.046	0.020	6.477
100	160	95.52	-4.09	1.42	-5.51	0.236	-0.026	-0.035	0.019	5.961
100	162	100.93	-4.27	1.45	-5.72	0.226	-0.044	-0.023	0.019	5.386
100	164	107.59	-3.67	1.14	-4.80	0.215	-0.041	-0.013	0.013	5.812
100	166	114.64	-3.13	1.01	-4.14	0.197	-0.044	-0.006	0.008	5.518
100	168	121.84	-2.88	0.81	-3.68	0.175	-0.040	-0.002	0.005	5.025
100	170	129.19	-2.92	0.63	-3.54	0.150	-0.037	0.001	0.002	4.557
100	172	136.52	-3.38	0.47	-3.85	-0.143	0.017	0.010	-0.007	3.982
100	174	144.17	-3.95	0.29	-4.24	-0.120	0.007	0.008	-0.003	3.672
100	176	152.27	-4.48	0.20	-4.68	-0.100	-0.004	0.007	0.001	3.480
100	178	160.63	-5.15	0.27	-5.42	-0.095	-0.014	0.011	0.006	3.054
100	180	169.65	-5.55	0.08	-5.62	-0.047	-0.011	-0.001	0.000	3.041
100	182	178.81	-6.19	0.01	-6.20	0.000	0.001	0.000	0.000	2.670
100	184	188.40	-6.78	0.08	-6.85	-0.001	0.002	0.000	0.000	2.573
100	186	200.15	-5.58	0.37	-5.94	0.004	0.002	0.002	0.000	4.119
100	188	212.05	-4.59	1.05	-5.64	0.026	0.014	0.001	-0.001	3.524
100	190	223.92	-3.98	1.78	-5.76	0.052	0.028	0.002	-0.003	2.575
100	192	236.03	-3.49	2.13	-5.62	0.067	0.030	-0.003	-0.003	2.132
102	138	84.61	-0.33	0.84	-1.17	0.241	0.049	-0.019	-0.008	10.347
102	140	82.84	-1.11	0.97	-2.08	0.237	0.052	-0.022	-0.009	10.037
102	142	81.63	-1.92	1.11	-3.03	0.237	0.053	-0.027	-0.011	9.756
102	144	81.03	-2.69	1.29	-3.98	0.242	0.051	-0.034	-0.012	9.511
102	146	81.07	-3.38	1.46	-4.83	0.246	0.046	-0.042	-0.012	9.273

Continued. . .

Table 1 contd. . .

Z	N	M_{gs}^{th}	E	E_{mac}	E_{mic}	β_{20}^{min}	β_{40}^{min}	β_{60}^{min}	β_{80}^{min}	Q_{alpha}
102	148	81.75	-3.98	1.46	-5.44	0.248	0.035	-0.047	-0.005	9.006
102	150	82.95	-4.60	1.53	-6.13	0.251	0.024	-0.051	0.003	8.532
102	152	84.70	-5.20	1.75	-6.95	0.254	0.014	-0.057	0.007	8.060
102	154	87.76	-5.00	1.74	-6.74	0.252	0.004	-0.056	0.014	8.359
102	156	91.37	-4.76	1.77	-6.53	0.252	-0.007	-0.053	0.021	7.989
102	158	95.34	-4.65	1.80	-6.45	0.248	-0.021	-0.048	0.025	7.445
102	160	99.64	-4.70	1.50	-6.20	0.237	-0.034	-0.035	0.021	6.862
102	162	104.19	-4.98	1.50	-6.48	0.228	-0.048	-0.024	0.020	6.249
102	164	110.15	-4.30	1.27	-5.58	0.217	-0.049	-0.015	0.014	6.792
102	166	116.50	-3.70	1.13	-4.83	0.202	-0.050	-0.008	0.009	6.480
102	168	123.13	-3.26	0.96	-4.23	0.184	-0.048	-0.002	0.006	6.065
102	170	129.87	-3.16	0.72	-3.88	0.157	-0.042	0.000	0.003	5.604
102	172	136.69	-3.40	0.47	-3.87	-0.146	0.017	0.011	-0.007	5.075
102	174	143.68	-3.90	0.28	-4.18	-0.124	0.006	0.008	-0.003	4.727
102	176	151.11	-4.36	0.22	-4.57	-0.105	-0.007	0.007	0.002	4.516
102	178	158.74	-5.03	0.31	-5.34	-0.098	-0.017	0.012	0.007	4.045
102	180	167.19	-5.29	0.09	-5.38	-0.053	-0.013	-0.001	0.000	4.138
102	182	175.78	-5.79	0.02	-5.81	0.000	0.001	0.000	0.000	3.706
102	184	184.73	-6.32	0.04	-6.35	0.000	0.001	0.000	0.000	3.492
102	186	195.69	-5.21	0.50	-5.71	-0.002	0.001	0.000	-0.002	4.867
102	188	206.90	-4.22	1.06	-5.28	0.018	0.010	0.001	-0.001	4.329
102	190	218.14	-3.56	1.76	-5.32	0.047	0.026	0.000	-0.004	3.667
102	192	229.57	-3.07	2.33	-5.40	0.072	0.035	-0.004	-0.002	3.217
104	140	97.94	-0.61	0.60	-1.21	0.238	0.036	-0.020	-0.009	10.905
104	142	95.90	-1.40	0.73	-2.13	0.236	0.038	-0.024	-0.010	10.633
104	144	94.46	-2.17	0.86	-3.03	0.239	0.036	-0.031	-0.011	10.408
104	146	93.63	-2.90	0.97	-3.88	0.243	0.030	-0.037	-0.009	10.173
104	148	93.34	-3.65	1.04	-4.69	0.245	0.020	-0.042	-0.003	9.848
104	150	93.54	-4.45	1.19	-5.64	0.248	0.009	-0.047	0.004	9.374
104	152	94.30	-5.22	1.46	-6.68	0.251	0.002	-0.053	0.009	8.932
104	154	96.41	-5.18	1.54	-6.71	0.250	-0.009	-0.051	0.016	9.283
104	156	99.02	-5.14	1.72	-6.86	0.249	-0.021	-0.050	0.023	8.837
104	158	102.04	-5.20	1.83	-7.03	0.247	-0.032	-0.046	0.027	8.245
104	160	105.41	-5.39	1.65	-7.04	0.239	-0.042	-0.036	0.025	7.646
104	162	109.11	-5.74	1.65	-7.39	0.231	-0.054	-0.025	0.023	7.047
104	164	114.37	-5.01	1.44	-6.45	0.221	-0.056	-0.017	0.017	7.754
104	166	120.06	-4.30	1.26	-5.55	0.203	-0.056	-0.010	0.012	7.489
104	168	126.07	-3.73	1.20	-4.93	0.191	-0.058	-0.001	0.008	7.143
104	170	132.17	-3.51	0.90	-4.41	0.164	-0.051	0.001	0.005	6.616
104	172	138.39	-3.62	0.78	-4.40	0.140	-0.049	0.006	0.002	6.094
104	174	144.81	-3.95	0.27	-4.22	-0.125	0.005	0.008	-0.004	5.696
104	176	151.47	-4.46	0.21	-4.66	-0.113	-0.005	0.004	0.000	5.367
104	178	158.47	-5.04	0.32	-5.36	-0.099	-0.020	0.012	0.008	4.930
104	180	166.31	-5.19	0.11	-5.29	-0.054	-0.015	-0.001	0.000	5.141
104	182	174.27	-5.61	0.19	-5.80	-0.042	-0.024	-0.008	-0.001	4.657
104	184	182.62	-6.03	0.06	-6.09	-0.001	0.000	0.000	0.000	4.417
104	186	192.88	-4.93	0.55	-5.48	-0.002	0.000	0.000	-0.001	5.724
104	188	203.40	-3.94	1.00	-4.93	0.009	0.007	0.000	-0.001	5.286
104	190	214.05	-3.19	1.63	-4.81	0.035	0.021	-0.001	-0.002	4.723
104	192	224.82	-2.67	2.18	-4.86	0.054	0.028	-0.004	-0.003	4.254
106	142	111.78	-0.96	0.44	-1.39	0.241	0.018	-0.026	-0.004	11.407
106	144	109.50	-1.72	0.53	-2.25	0.240	0.015	-0.030	-0.003	11.184
106	146	107.75	-2.55	0.69	-3.24	0.243	0.009	-0.036	0.000	10.866
106	148	106.49	-3.44	0.84	-4.28	0.245	0.001	-0.040	0.005	10.444
106	150	105.73	-4.39	1.07	-5.46	0.247	-0.006	-0.045	0.010	9.965
106	152	105.58	-5.26	1.32	-6.58	0.248	-0.011	-0.050	0.013	9.615
106	154	106.68	-5.43	1.51	-6.94	0.248	-0.022	-0.049	0.020	9.955
106	156	108.33	-5.56	1.79	-7.36	0.249	-0.032	-0.048	0.027	9.495
106	158	110.38	-5.80	1.95	-7.75	0.246	-0.042	-0.045	0.031	8.930
106	160	112.88	-6.08	1.87	-7.95	0.240	-0.051	-0.036	0.029	8.423
106	162	115.72	-6.52	1.84	-8.36	0.233	-0.061	-0.025	0.026	7.886
106	164	120.27	-5.73	1.63	-7.36	0.223	-0.064	-0.016	0.019	8.734
106	166	125.29	-4.93	1.57	-6.50	0.213	-0.067	-0.008	0.015	8.501
106	168	130.62	-4.29	1.50	-5.78	0.198	-0.069	0.001	0.010	8.135
106	170	136.14	-3.91	1.16	-5.08	0.172	-0.061	0.004	0.006	7.646
106	172	141.67	-3.96	0.82	-4.78	0.139	-0.052	0.006	0.003	7.075
106	174	147.39	-4.26	0.49	-4.76	0.108	-0.039	0.005	0.001	6.570

Continued. . .

Table 1 contd. . .

Z	N	M_{gs}^{th}	E	E_{mac}	E_{mic}	β_{20}^{min}	β_{40}^{min}	β_{60}^{min}	β_{80}^{min}	Q_{alpha}
106	176	153.46	-4.63	0.62	-5.25	0.095	-0.045	0.011	0.000	6.227
106	178	159.84	-5.12	0.31	-5.43	-0.098	-0.021	0.012	0.008	5.944
106	180	166.98	-5.25	0.10	-5.35	-0.052	-0.016	-0.002	0.000	6.087
106	182	174.32	-5.58	0.01	-5.59	0.000	0.000	0.000	0.000	5.589
106	184	182.03	-5.94	0.02	-5.95	0.000	0.000	0.000	0.000	5.338
106	186	191.61	-4.82	0.38	-5.20	-0.001	0.001	0.001	0.000	6.571
106	188	201.50	-3.77	0.84	-4.60	-0.003	0.008	-0.002	0.001	6.200
106	190	211.58	-2.90	1.43	-4.33	0.022	0.014	-0.003	-0.001	5.757
106	192	221.70	-2.37	2.14	-4.51	0.050	0.027	-0.005	-0.002	5.225
108	144	126.16	-1.31	0.40	-1.71	0.243	-0.013	-0.026	0.001	11.960
108	146	123.55	-2.17	0.49	-2.66	0.240	-0.012	-0.029	0.006	11.621
108	148	121.44	-3.09	0.60	-3.69	0.240	-0.014	-0.032	0.008	11.266
108	150	119.83	-4.08	0.86	-4.94	0.242	-0.021	-0.037	0.012	10.914
108	152	118.87	-4.97	1.00	-5.97	0.242	-0.022	-0.041	0.013	10.715
108	154	119.00	-5.30	1.24	-6.53	0.243	-0.034	-0.039	0.020	10.994
108	156	119.69	-5.60	1.53	-7.13	0.243	-0.044	-0.037	0.027	10.581
108	158	120.79	-6.00	1.82	-7.83	0.242	-0.053	-0.037	0.030	10.039
108	160	122.30	-6.50	1.87	-8.37	0.238	-0.062	-0.027	0.029	9.501
108	162	124.18	-7.13	2.03	-9.17	0.233	-0.071	-0.021	0.029	8.869
108	164	127.94	-6.36	1.88	-8.24	0.225	-0.074	-0.013	0.023	9.795
108	166	132.25	-5.52	1.83	-7.35	0.218	-0.076	-0.005	0.019	9.554
108	168	136.91	-4.80	1.80	-6.60	0.205	-0.079	0.003	0.012	9.193
108	170	141.81	-4.29	1.50	-5.79	0.180	-0.072	0.008	0.007	8.765
108	172	146.58	-4.37	0.75	-5.12	0.133	-0.051	0.006	0.003	8.013
108	174	151.54	-4.69	0.58	-5.27	0.106	-0.045	0.006	0.001	7.445
108	176	156.89	-5.06	0.70	-5.76	0.096	-0.049	0.013	0.000	7.078
108	178	162.79	-5.30	0.26	-5.56	-0.094	-0.019	0.011	0.006	6.905
108	180	169.18	-5.47	0.09	-5.56	-0.046	-0.015	-0.002	0.000	6.915
108	182	175.85	-5.76	0.01	-5.78	0.000	-0.001	0.000	0.000	6.446
108	184	182.95	-6.04	0.01	-6.05	0.000	0.000	0.000	0.000	6.203
108	186	191.89	-4.86	0.10	-4.97	-0.002	0.000	0.000	0.000	7.427
108	188	201.18	-3.72	0.53	-4.25	-0.002	0.001	-0.001	0.000	7.143
108	190	210.70	-2.74	1.00	-3.74	0.007	0.009	-0.002	-0.001	6.766
108	192	220.20	-2.14	2.11	-4.25	0.046	0.026	-0.005	-0.002	6.191
110	146	141.58	-1.19	0.21	-1.41	0.220	0.008	-0.026	0.001	12.994
110	148	138.71	-2.06	0.32	-2.39	0.228	-0.002	-0.029	0.005	12.735
110	150	136.32	-3.02	0.47	-3.49	0.235	-0.009	-0.033	0.008	12.458
110	152	134.55	-3.91	0.71	-4.63	0.239	-0.016	-0.038	0.011	12.293
110	154	133.94	-4.19	0.88	-5.06	0.236	-0.031	-0.034	0.016	12.648
110	156	133.83	-4.50	1.12	-5.62	0.234	-0.044	-0.030	0.021	12.405
110	158	134.05	-5.01	1.37	-6.38	0.232	-0.057	-0.024	0.023	11.935
110	160	134.59	-5.71	1.60	-7.31	0.228	-0.067	-0.017	0.023	11.369
110	162	135.47	-6.56	1.91	-8.47	0.226	-0.077	-0.012	0.025	10.741
110	164	138.18	-6.09	1.91	-7.99	0.217	-0.081	-0.002	0.019	11.573
110	166	141.49	-5.49	1.99	-7.48	0.211	-0.084	0.006	0.015	11.123
110	168	145.22	-4.95	2.14	-7.08	0.202	-0.089	0.013	0.009	10.546
110	170	149.23	-4.58	0.78	-5.36	0.147	-0.052	0.001	0.006	9.896
110	172	153.13	-4.80	0.67	-5.47	0.127	-0.049	0.006	0.003	8.886
110	174	157.33	-5.15	0.55	-5.70	0.095	-0.045	0.007	0.001	8.329
110	176	161.96	-5.51	0.72	-6.23	0.093	-0.050	0.015	0.000	7.990
110	178	167.29	-5.60	0.18	-5.78	-0.085	-0.015	0.010	0.005	7.978
110	180	172.88	-5.86	0.07	-5.92	-0.037	-0.013	-0.002	0.000	7.670
110	182	178.88	-6.13	0.01	-6.14	-0.002	0.002	0.001	0.000	7.273
110	184	185.35	-6.32	0.02	-6.34	-0.002	0.001	0.000	0.000	7.076
110	186	193.58	-5.16	0.01	-5.18	-0.001	0.000	0.000	0.001	8.204
110	188	202.31	-3.89	0.02	-3.91	0.000	0.000	0.000	0.000	7.998
110	190	211.29	-2.76	0.45	-3.22	-0.002	0.002	-0.001	0.000	7.681
110	192	220.27	-2.00	1.99	-4.00	0.045	0.024	-0.005	-0.002	7.156
112	148	157.46	-1.17	0.12	-1.28	0.211	0.005	-0.025	0.002	13.458
112	150	154.38	-2.01	0.23	-2.24	0.223	-0.003	-0.029	0.006	13.246
112	152	151.87	-2.85	0.42	-3.27	0.233	-0.010	-0.034	0.009	13.121
112	154	150.48	-3.11	0.53	-3.64	0.222	-0.028	-0.028	0.012	13.506
112	156	149.51	-3.50	0.75	-4.25	0.218	-0.044	-0.022	0.014	13.136
112	158	148.83	-4.12	1.05	-5.16	0.217	-0.058	-0.014	0.016	12.576
112	160	148.46	-4.95	1.46	-6.41	0.218	-0.071	-0.008	0.020	11.987
112	162	148.45	-5.93	1.95	-7.89	0.221	-0.083	-0.004	0.024	11.441
112	164	150.12	-5.74	1.98	-7.72	0.208	-0.087	0.003	0.016	12.224

Continued. . .

Table 1 contd. . .

Z	N	M_{gs}^{th}	E	E_{mac}	E_{mic}	β_{20}^{min}	β_{40}^{min}	β_{60}^{min}	β_{80}^{min}	Q_{alpha}
112	166	152.46	-5.36	2.30	-7.65	0.204	-0.093	0.015	0.013	11.860
112	168	155.27	-4.98	2.43	-7.42	0.193	-0.095	0.021	0.009	11.356
112	170	158.33	-4.84	0.87	-5.71	0.145	-0.057	0.006	0.005	10.684
112	172	161.43	-5.11	0.84	-5.95	0.129	-0.056	0.011	0.003	9.774
112	174	164.87	-5.49	0.56	-6.05	0.094	-0.045	0.010	0.001	9.324
112	176	168.80	-5.84	0.77	-6.61	0.089	-0.052	0.016	-0.001	9.042
112	178	173.31	-6.03	0.10	-6.13	-0.073	-0.009	0.008	0.003	8.928
112	180	178.07	-6.41	0.01	-6.42	0.004	-0.002	0.000	0.000	8.357
112	182	183.38	-6.65	0.01	-6.67	0.000	0.000	0.001	0.000	8.074
112	184	189.26	-6.74	0.01	-6.75	0.000	0.000	0.000	0.000	7.964
112	186	196.82	-5.56	0.01	-5.57	-0.001	0.000	0.000	0.000	9.040
112	188	204.87	-4.29	0.01	-4.30	0.000	0.002	0.001	0.000	8.864
112	190	213.23	-3.09	0.01	-3.11	0.000	0.000	0.000	0.000	8.493
112	192	221.86	-2.01	0.01	-2.02	0.000	0.000	0.000	0.000	8.147
114	150	173.88	-1.15	-0.06	-1.08	0.231	0.008	-0.023	0.007	13.996
114	152	170.63	-1.93	0.11	-2.04	0.237	-0.002	-0.029	0.009	13.828
114	154	168.45	-2.20	0.27	-2.47	0.212	-0.027	-0.021	0.008	14.153
114	156	166.58	-2.70	0.51	-3.20	0.200	-0.044	-0.012	0.010	13.675
114	158	165.05	-3.40	0.84	-4.24	0.201	-0.058	-0.005	0.012	13.116
114	160	163.81	-4.33	1.35	-5.68	0.206	-0.073	-0.001	0.017	12.555
114	162	163.01	-5.34	1.98	-7.31	0.213	-0.087	0.002	0.023	12.127
114	164	163.65	-5.41	2.13	-7.55	0.202	-0.091	0.012	0.017	12.771
114	166	165.08	-5.20	2.48	-7.68	0.196	-0.098	0.021	0.013	12.532
114	168	166.96	-5.00	2.93	-7.93	0.191	-0.104	0.031	0.009	12.078
114	170	169.24	-4.90	1.43	-6.33	0.151	-0.073	0.018	0.005	11.544
114	172	171.55	-5.23	0.22	-5.45	-0.120	0.023	0.003	-0.008	10.798
114	174	174.18	-5.70	0.37	-6.06	0.086	-0.037	0.008	0.001	10.321
114	176	177.37	-6.06	0.05	-6.11	-0.074	-0.002	0.005	0.001	10.070
114	178	180.60	-6.82	0.01	-6.83	0.000	0.000	0.000	0.000	9.608
114	180	184.90	-6.94	0.01	-6.95	0.001	0.000	0.000	0.000	9.167
114	182	189.61	-7.09	0.01	-7.10	0.000	0.000	0.000	0.000	9.113
114	184	194.90	-7.07	0.01	-7.09	0.000	0.000	0.000	0.000	9.088
114	186	201.76	-5.90	0.01	-5.91	-0.001	0.001	0.001	0.000	10.067
114	188	209.12	-4.62	0.01	-4.63	0.000	0.000	0.000	0.000	9.878
114	190	216.80	-3.42	0.01	-3.43	0.000	0.000	0.000	0.000	9.511
114	192	224.76	-2.34	0.01	-2.35	0.000	0.001	0.000	0.000	9.109
116	152	190.84	-1.14	-0.14	-1.00	0.240	0.004	-0.026	0.008	14.533
116	154	187.96	-1.32	0.03	-1.35	0.213	-0.024	-0.015	0.008	14.900
116	156	185.22	-1.91	0.49	-2.41	0.192	-0.051	-0.002	0.007	14.346
116	158	182.78	-2.75	0.97	-3.72	0.192	-0.066	0.004	0.011	13.769
116	160	180.71	-3.74	1.45	-5.18	0.196	-0.078	0.007	0.017	13.243
116	162	179.14	-4.76	1.99	-6.75	0.204	-0.089	0.006	0.024	12.900
116	164	178.77	-5.08	2.20	-7.28	0.192	-0.094	0.017	0.016	13.336
116	166	179.28	-5.04	2.60	-7.63	0.186	-0.100	0.027	0.013	13.207
116	168	180.28	-4.99	3.03	-8.01	0.181	-0.105	0.035	0.009	12.783
116	170	181.70	-5.01	0.11	-5.11	-0.111	0.017	0.002	-0.004	12.307
116	172	183.07	-5.55	0.14	-5.68	-0.115	0.018	0.005	-0.007	11.401
116	174	185.12	-5.87	0.05	-5.92	-0.092	0.005	0.004	-0.002	11.140
116	176	187.52	-6.29	0.05	-6.34	-0.078	-0.004	0.006	0.000	10.920
116	178	190.43	-6.67	0.09	-6.76	-0.075	-0.009	0.010	0.003	10.632
116	180	193.97	-6.85	0.01	-6.86	0.002	0.000	0.000	0.000	10.712
116	182	198.03	-6.94	0.01	-6.95	0.001	0.000	0.000	0.000	10.703
116	184	202.68	-6.86	0.01	-6.87	-0.001	0.000	0.000	0.000	10.647
116	186	208.82	-5.71	0.01	-5.73	0.000	0.001	0.000	0.000	11.498
116	188	215.48	-4.46	0.01	-4.47	0.000	0.000	0.000	0.000	11.296
116	190	222.46	-3.28	0.01	-3.29	0.000	0.001	0.000	0.000	10.910
116	192	229.72	-2.22	0.01	-2.23	0.000	0.000	0.000	0.000	10.489
118	154	208.87	-0.60	-0.23	-0.37	0.219	-0.018	-0.011	0.008	15.605
118	156	205.37	-1.17	0.41	-1.58	0.177	-0.050	0.004	0.006	14.990
118	158	202.18	-1.99	0.75	-2.74	0.182	-0.061	0.007	0.009	14.537
118	160	199.43	-2.90	1.07	-3.97	0.190	-0.071	0.007	0.013	14.229
118	162	197.15	-3.87	1.64	-5.50	0.203	-0.083	0.007	0.022	14.013
118	164	195.98	-4.24	1.84	-6.08	0.186	-0.087	0.017	0.015	14.415
118	166	195.72	-4.22	2.11	-6.33	0.175	-0.091	0.025	0.010	14.518
118	168	195.78	-4.37	0.03	-4.40	-0.107	0.009	0.004	-0.002	14.072
118	170	195.79	-5.06	0.06	-5.12	-0.116	0.012	0.006	-0.004	13.078
118	172	196.46	-5.57	0.11	-5.68	-0.122	0.015	0.008	-0.006	12.335

Continued. . .

Table 1 contd. . .

Z	N	M_{gs}^{th}	E	E_{mac}	E_{mic}	β_{20}^{min}	β_{40}^{min}	β_{60}^{min}	β_{80}^{min}	Q_{alpha}
118	174	197.76	-5.91	0.38	-6.29	0.081	-0.038	0.011	0.001	12.270
118	176	199.63	-6.16	0.06	-6.23	-0.090	-0.008	0.008	0.002	12.088
118	178	201.86	-6.49	0.15	-6.64	-0.087	-0.014	0.012	0.005	11.915
118	180	204.92	-6.45	0.06	-6.50	-0.037	-0.013	-0.002	0.000	12.069
118	182	208.38	-6.44	0.01	-6.45	0.000	0.000	0.000	0.000	11.983
118	184	212.40	-6.29	0.01	-6.31	0.000	0.000	0.000	0.000	11.949
118	186	217.82	-5.19	0.01	-5.20	-0.001	0.000	0.000	0.000	12.707
118	188	223.76	-3.96	0.01	-3.97	0.000	-0.001	0.000	0.000	12.519
118	190	230.04	-2.81	0.01	-2.82	-0.001	0.000	0.000	0.000	12.134
118	192	236.11	-2.26	1.32	-3.58	-0.404	0.006	0.010	-0.010	11.224
120	156	225.79	-1.71	0.41	-2.12	-0.432	0.036	0.015	-0.015	14.491
120	158	222.21	-2.14	0.53	-2.68	-0.435	0.039	0.016	-0.016	14.408
120	160	219.14	-2.61	0.65	-3.27	-0.439	0.043	0.016	-0.016	14.532
120	162	216.58	-3.10	0.77	-3.87	-0.442	0.048	0.016	-0.016	14.729
120	164	214.62	-3.51	0.89	-4.40	-0.444	0.052	0.016	-0.016	15.047
120	166	213.60	-3.51	1.03	-4.53	-0.451	0.055	0.016	-0.017	15.195
120	168	212.38	-4.20	0.02	-4.22	-0.123	0.012	0.008	-0.001	14.239
120	170	211.64	-4.91	0.05	-4.96	-0.130	0.013	0.010	-0.003	13.437
120	172	211.58	-5.41	0.11	-5.53	-0.136	0.016	0.013	-0.007	13.372
120	174	212.27	-5.66	0.60	-6.25	0.084	-0.047	0.016	0.003	13.390
120	176	213.43	-5.89	0.92	-6.81	0.085	-0.056	0.023	0.003	13.241
120	178	215.19	-5.99	0.14	-6.12	-0.092	-0.013	0.014	0.005	13.138
120	180	217.64	-5.85	0.09	-5.94	-0.036	-0.018	-0.004	0.000	13.347
120	182	220.46	-5.78	0.01	-5.79	0.000	0.000	0.000	0.000	13.114
120	184	223.87	-5.56	0.01	-5.57	0.000	0.000	0.000	0.000	13.069
120	186	228.56	-4.48	0.01	-4.49	0.000	0.000	0.000	0.000	13.730
120	188	233.81	-3.26	0.39	-3.65	0.016	0.005	0.004	0.001	13.570
120	190	238.78	-2.74	1.08	-3.82	-0.407	0.006	0.013	-0.012	12.592
120	192	243.80	-2.58	1.10	-3.68	-0.413	0.009	0.010	-0.011	11.334
122	158	244.04	-2.01	0.06	-2.07	-0.446	0.044	0.009	-0.016	15.830
122	160	240.10	-2.60	0.19	-2.79	-0.449	0.047	0.010	-0.016	15.463
122	162	236.67	-3.20	0.32	-3.52	-0.452	0.052	0.011	-0.016	15.109
122	164	233.85	-3.73	0.45	-4.18	-0.456	0.056	0.011	-0.016	14.845
122	166	231.92	-3.88	0.61	-4.49	-0.464	0.059	0.012	-0.017	14.873
122	168	230.59	-3.95	0.00	-3.95	-0.143	0.016	0.009	0.000	14.566
122	170	229.10	-4.68	0.03	-4.71	-0.145	0.015	0.013	-0.003	14.292
122	172	228.30	-5.21	0.11	-5.31	-0.147	0.016	0.016	-0.006	14.233
122	174	228.52	-5.19	0.05	-5.25	-0.135	0.009	0.015	-0.002	14.512
122	176	229.19	-5.21	0.04	-5.25	-0.116	-0.003	0.013	0.002	14.494
122	178	230.26	-5.29	0.17	-5.46	-0.104	-0.017	0.014	0.007	14.402
122	180	232.09	-5.06	0.14	-5.20	-0.038	-0.022	-0.006	0.000	14.478
122	182	234.28	-4.93	0.01	-4.94	0.000	0.000	0.000	0.000	14.218
122	184	237.06	-4.64	0.01	-4.65	0.000	0.000	0.000	0.000	14.171
122	186	240.99	-3.64	0.63	-4.27	0.014	0.003	0.013	0.002	14.696
122	188	244.94	-3.04	0.15	-3.18	-0.189	-0.001	0.017	0.007	13.958
122	190	249.04	-2.71	0.23	-2.94	-0.199	-0.006	0.020	0.008	12.808
122	192	253.50	-2.43	0.79	-3.22	-0.420	0.010	0.007	-0.010	12.296
124	160	262.80	-2.34	-0.33	-2.02	-0.459	0.050	0.007	-0.014	16.330
124	162	258.56	-3.01	-0.19	-2.81	-0.462	0.054	0.008	-0.015	16.043
124	164	254.92	-3.62	-0.05	-3.56	-0.465	0.057	0.009	-0.016	15.820
124	166	252.10	-3.92	0.10	-4.02	-0.473	0.061	0.010	-0.016	15.825
124	168	250.51	-3.51	0.20	-3.71	-0.477	0.064	0.006	-0.016	16.163
124	170	248.31	-4.22	-0.04	-4.19	-0.163	0.019	0.012	-0.001	15.293
124	172	246.78	-4.75	0.04	-4.79	-0.163	0.017	0.017	-0.005	15.256
124	174	246.39	-4.64	0.02	-4.66	-0.167	0.017	0.017	-0.002	15.663
124	176	246.37	-4.63	0.15	-4.78	-0.211	0.042	0.010	-0.004	15.421
124	178	246.52	-4.92	0.30	-5.22	-0.230	0.050	0.011	-0.007	14.901
124	180	247.70	-4.65	0.32	-4.97	-0.241	0.048	0.015	-0.008	15.017
124	182	249.62	-4.08	0.27	-4.35	-0.241	0.043	0.017	-0.007	15.101
124	184	251.77	-3.73	1.57	-5.30	0.018	-0.001	0.029	-0.012	15.067
124	186	254.45	-3.30	0.04	-3.34	-0.194	0.007	0.016	0.009	14.966
124	188	257.40	-3.02	0.13	-3.15	-0.200	-0.002	0.020	0.010	13.984
124	190	260.75	-2.77	0.22	-2.98	-0.205	-0.007	0.023	0.010	13.382
124	192	264.52	-2.51	0.37	-2.87	-0.212	-0.015	0.025	0.013	13.053
126	162	281.99	-2.77	-0.75	-2.02	-0.471	0.056	0.005	-0.013	16.762
126	164	277.54	-3.44	-0.61	-2.83	-0.474	0.060	0.006	-0.013	16.547
126	166	273.85	-3.88	-0.45	-3.42	-0.482	0.064	0.008	-0.015	16.507

Continued. . .

Table 1 contd. . .

Z	N	M_{gs}^{th}	E	E_{mac}	E_{mic}	β_{20}^{min}	β_{40}^{min}	β_{60}^{min}	β_{80}^{min}	Q_{alpha}
126	168	271.43	-3.57	-0.34	-3.23	-0.488	0.067	0.004	-0.015	16.898
126	170	269.00	-3.78	-0.12	-3.66	-0.180	0.021	0.014	0.000	16.064
126	172	266.79	-4.28	-0.05	-4.23	-0.178	0.019	0.018	-0.003	16.052
126	174	265.48	-4.36	-0.06	-4.30	-0.195	0.027	0.016	-0.001	16.280
126	176	264.56	-4.54	-0.01	-4.53	-0.214	0.037	0.014	-0.002	15.754
126	178	264.04	-4.80	0.09	-4.88	-0.229	0.044	0.014	-0.004	15.250
126	180	264.51	-4.53	0.10	-4.63	-0.238	0.041	0.019	-0.005	15.569
126	182	265.70	-4.00	0.06	-4.07	-0.236	0.034	0.021	-0.002	15.580
126	184	267.32	-3.50	-0.01	-3.49	-0.220	0.021	0.020	0.004	15.276
126	186	269.19	-3.19	0.00	-3.19	-0.211	0.008	0.020	0.009	14.993
126	188	271.41	-2.96	0.10	-3.06	-0.212	-0.002	0.023	0.011	14.537
126	190	274.01	-2.78	0.26	-3.04	-0.214	-0.010	0.027	0.014	14.190
126	192	277.07	-2.57	0.36	-2.93	-0.220	-0.016	0.028	0.016	13.896

Table 2. Saddle point properties

For the isotopes of the elements $Z=98-126$, tabulates the saddle point masses, total energies, macroscopic and microscopic energies as well as saddle point deformations.

Z	The atomic number
A	The mass number
m_{sp}^{th}	The mass excess in MeV
E	The total energy in MeV
E_{mac}	The macroscopic energy in MeV
E_{mic}	The microscopic energy in MeV
$\beta_{20}^{sp} \div \beta_{80}^{sp}$	The saddle point deformations
Q_{alpha}	Theoretical Q -value in MeV

Table 1
Calculated Saddle Point Masses and Deformations.

Z	N	M_{sp}^{th}	E	E_{mac}	E_{mic}	β_{20}^{sp}	$\gamma^{sp}(^\circ)$	β_{40}^{sp}	β_{42}^{sp}	β_{44}^{sp}	β_{60}^{sp}	β_{80}^{sp}
98	134	61.77	2.33	1.64	0.68	0.393	7.3	-0.010	0.009	-0.003	-0.014	-0.019
98	136	61.12	2.12	2.18	-0.06	0.412	5.6	-0.030	0.015	0.003	-0.022	-0.015
98	138	61.49	2.35	2.18	0.18	0.421	2.7	-0.030	0.008	0.003	-0.026	-0.008
98	140	62.69	2.82	2.23	0.59	0.440	0.0	-0.030	0.000	-0.002	-0.025	0.001
98	142	64.26	3.10	2.45	0.65	0.475	8.5	-0.010	0.017	0.022	-0.011	0.001
98	144	66.18	3.15	2.55	0.61	0.510	11.3	0.000	0.000	0.023	0.006	-0.002
98	146	68.18	2.75	2.85	-0.10	0.526	14.3	0.030	0.002	0.025	0.020	0.005
98	148	70.79	2.43	2.91	-0.48	0.526	14.3	0.030	0.003	0.025	0.018	0.007
98	150	74.09	2.26	2.71	-0.45	0.500	16.3	0.030	0.004	0.019	0.003	0.011
98	152	77.80	2.00	2.65	-0.66	0.490	16.6	0.030	0.005	0.015	0.001	0.012
98	154	81.89	1.61	2.77	-1.16	0.500	16.3	0.040	0.007	0.014	0.006	0.012
98	156	86.41	1.17	2.77	-1.60	0.517	14.6	0.040	0.006	0.018	0.006	0.008
98	158	91.60	0.90	2.84	-1.94	0.536	14.0	0.040	-0.001	0.021	0.003	0.003
98	160	97.28	0.66	2.99	-2.33	0.573	12.1	0.030	-0.008	0.024	-0.004	-0.004
98	162	103.77	0.78	3.01	-2.24	0.575	13.1	0.030	-0.005	0.018	-0.009	-0.004
98	164	110.67	0.85	2.91	-2.06	0.582	11.9	0.030	-0.006	0.012	-0.012	-0.002
98	166	118.04	0.94	2.88	-1.94	0.582	11.9	0.030	-0.006	0.007	-0.013	-0.001
98	168	125.77	0.97	2.82	-1.86	0.590	10.7	0.030	-0.007	0.003	-0.013	0.001
98	170	133.94	1.01	2.85	-1.84	0.592	11.7	0.040	-0.005	0.002	-0.015	0.003
98	172	141.21	-0.27	1.10	-1.37	0.280	0.0	0.020	0.000	0.000	0.006	0.018
98	174	150.37	-0.06	1.04	-1.11	0.270	0.0	0.020	0.000	0.000	0.013	0.014
98	176	159.70	-0.09	1.32	-1.41	0.297	19.7	0.020	-0.009	-0.005	0.012	0.007
98	178	169.26	-0.28	1.35	-1.63	0.307	19.0	0.020	-0.007	-0.006	0.013	0.004
98	180	179.14	-0.53	1.46	-1.99	0.320	20.1	0.030	-0.004	-0.005	0.011	0.002
98	182	189.35	-0.84	1.58	-2.41	0.323	21.8	0.040	0.001	-0.001	0.010	0.000
98	184	199.83	-1.24	1.51	-2.74	0.345	16.9	0.030	-0.003	-0.007	0.008	-0.006
98	186	210.79	-1.52	1.55	-3.07	0.369	12.5	0.010	-0.007	-0.007	0.004	-0.012
98	188	222.04	-1.88	1.11	-2.99	0.199	40.9	0.040	-0.003	-0.013	0.015	0.005
98	190	233.68	-2.20	1.42	-3.62	0.190	18.4	0.060	0.005	-0.002	0.029	0.002
98	192	245.59	-2.58	1.60	-4.18	0.197	14.7	0.070	0.006	-0.002	0.027	-0.001
100	136	74.40	2.50	1.64	0.86	0.410	0.0	-0.030	0.000	0.000	-0.019	-0.014
100	138	73.91	2.73	1.71	1.02	0.420	0.0	-0.030	0.000	0.000	-0.022	-0.007
100	140	73.86	2.81	2.14	0.67	0.509	19.5	0.060	-0.016	0.007	0.009	-0.003
100	142	74.33	2.84	2.48	0.35	0.488	22.9	0.070	-0.013	0.009	0.003	-0.001
100	144	75.28	2.78	2.45	0.32	0.488	22.9	0.060	-0.014	0.008	-0.001	0.002
100	146	76.80	2.73	2.26	0.47	0.490	20.3	0.050	-0.011	0.011	-0.001	0.004
100	148	78.70	2.52	2.26	0.26	0.487	19.2	0.050	-0.001	0.013	0.002	0.008
100	150	81.04	2.22	2.22	0.00	0.484	18.1	0.040	0.002	0.014	0.002	0.011
100	152	83.83	1.85	2.24	-0.39	0.481	16.9	0.050	0.004	0.012	0.005	0.013
100	154	87.06	1.41	2.34	-0.93	0.481	16.9	0.060	0.007	0.008	0.004	0.014
100	156	90.76	0.95	2.57	-1.63	0.474	18.4	0.070	0.011	0.004	0.001	0.014
100	158	95.01	0.54	2.61	-2.07	0.430	17.6	0.080	0.007	-0.013	-0.005	0.019
100	160	99.66	0.06	2.71	-2.65	0.381	13.7	0.090	0.004	-0.023	-0.010	0.021
100	162	105.43	0.22	2.50	-2.28	0.592	11.7	0.030	-0.002	0.020	-0.008	-0.005
100	164	111.61	0.34	2.46	-2.11	0.585	12.9	0.040	-0.001	0.015	-0.009	-0.003
100	166	118.17	0.40	2.37	-1.97	0.592	11.7	0.040	-0.001	0.011	-0.012	-0.003
100	168	125.17	0.45	2.40	-1.95	0.594	12.6	0.050	-0.001	0.007	-0.012	0.000
100	170	132.57	0.47	2.32	-1.85	0.602	11.5	0.050	-0.001	0.005	-0.013	0.002
100	172	139.41	-0.50	1.05	-1.55	0.290	0.0	0.020	0.000	0.000	0.004	0.020
100	174	147.86	-0.27	0.98	-1.24	0.280	0.0	0.020	0.000	0.000	0.008	0.016
100	176	156.63	-0.12	0.94	-1.07	0.270	0.0	0.020	0.000	0.000	0.016	0.012
100	178	165.64	-0.13	1.03	-1.16	0.270	0.0	0.030	0.000	0.000	0.019	0.010
100	180	174.82	-0.37	1.38	-1.74	0.314	22.5	0.030	-0.007	-0.005	0.014	-0.001
100	182	184.27	-0.73	1.41	-2.14	0.318	24.2	0.030	-0.003	-0.001	0.013	-0.002
100	184	194.05	-1.13	1.43	-2.56	0.313	26.6	0.030	0.001	0.001	0.012	-0.004
100	186	204.27	-1.45	1.38	-2.84	0.361	14.4	0.020	-0.007	-0.009	0.005	-0.011
100	188	214.78	-1.85	1.15	-3.01	0.194	34.5	0.050	-0.003	-0.008	0.017	0.005
100	190	225.85	-2.05	1.31	-3.36	0.180	19.4	0.060	0.003	-0.003	0.026	0.003
100	192	237.11	-2.41	1.29	-3.70	0.175	13.2	0.060	0.005	-0.002	0.028	0.000
102	138	87.37	2.43	1.70	0.72	0.500	19.9	0.080	-0.010	0.006	0.013	0.000
102	140	86.38	2.43	2.06	0.38	0.470	23.9	0.080	-0.006	0.006	-0.002	-0.003
102	142	85.94	2.40	2.13	0.26	0.470	23.9	0.080	-0.010	0.006	-0.001	0.000
102	144	85.98	2.27	2.32	-0.05	0.483	24.5	0.080	-0.012	0.008	-0.001	0.002
102	146	86.61	2.16	2.39	-0.22	0.492	24.0	0.080	-0.012	0.007	0.001	0.006

Continued...

Table 1 contd. . .

Z	N	M_{sp}^{th}	E	E_{mac}	E_{mic}	β_{20}^{sp}	$\gamma^{sp} (^{\circ})$	β_{40}^{sp}	β_{42}^{sp}	β_{44}^{sp}	β_{60}^{sp}	β_{80}^{sp}
102	148	87.80	2.07	2.35	-0.28	0.498	22.5	0.080	-0.010	0.005	0.003	0.011
102	150	89.47	1.92	2.31	-0.39	0.494	21.4	0.080	-0.004	0.005	0.002	0.012
102	152	91.46	1.57	2.11	-0.55	0.487	19.2	0.070	0.005	0.009	0.005	0.012
102	154	93.91	1.15	2.20	-1.05	0.474	18.4	0.080	0.009	0.004	0.002	0.011
102	156	96.64	0.51	2.35	-1.84	0.424	19.3	0.080	0.002	-0.016	-0.006	0.020
102	158	100.15	0.15	2.22	-2.07	0.371	14.0	0.080	-0.003	-0.022	-0.013	0.023
102	160	104.28	-0.06	2.61	-2.67	0.388	11.9	0.100	0.004	-0.021	-0.006	0.023
102	162	108.83	-0.34	2.66	-2.99	0.398	11.6	0.100	0.003	-0.022	-0.008	0.024
102	164	113.91	-0.55	2.52	-3.07	0.410	12.7	0.090	0.002	-0.025	-0.010	0.023
102	166	119.70	-0.50	2.44	-2.94	0.420	12.4	0.090	-0.003	-0.024	-0.014	0.019
102	168	125.92	-0.48	2.20	-2.68	0.420	12.4	0.080	-0.009	-0.022	-0.017	0.015
102	170	132.49	-0.54	2.04	-2.58	0.425	15.0	0.060	-0.010	-0.026	-0.014	0.008
102	172	139.34	-0.75	1.03	-1.79	0.300	0.0	0.020	0.000	0.000	0.002	0.025
102	174	147.16	-0.41	0.86	-1.27	0.280	0.0	0.010	0.000	0.000	0.008	0.017
102	176	155.21	-0.26	0.86	-1.12	0.280	0.0	0.010	0.000	0.000	0.014	0.013
102	178	163.56	-0.21	0.87	-1.08	0.270	0.0	0.020	0.000	0.000	0.019	0.010
102	180	172.20	-0.28	0.91	-1.18	0.270	2.1	0.020	-0.003	0.000	0.023	0.006
102	182	181.03	-0.54	1.28	-1.81	0.313	26.6	0.020	-0.006	0.002	0.014	-0.003
102	184	190.14	-0.90	1.28	-2.18	0.304	27.4	0.030	-0.002	0.002	0.014	-0.001
102	186	199.64	-1.25	1.28	-2.54	0.300	30.0	0.030	0.002	-0.001	0.010	-0.004
102	188	209.47	-1.64	1.20	-2.84	0.261	32.5	0.040	0.005	-0.002	0.012	-0.002
102	190	219.82	-1.88	1.20	-3.08	0.171	20.6	0.060	0.002	-0.003	0.023	0.004
102	192	230.49	-2.15	1.17	-3.32	0.153	11.3	0.060	0.003	-0.004	0.025	0.003
104	140	100.50	1.95	1.68	0.27	0.453	22.0	0.090	-0.009	-0.016	0.002	-0.001
104	142	99.18	1.88	2.07	-0.18	0.457	23.2	0.100	-0.009	-0.016	0.003	0.002
104	144	98.28	1.65	2.54	-0.90	0.448	23.7	0.110	-0.011	-0.022	0.002	0.006
104	146	97.96	1.43	2.45	-1.02	0.439	24.2	0.100	-0.015	-0.022	-0.003	0.006
104	148	98.40	1.41	2.30	-0.88	0.431	21.8	0.100	-0.012	-0.021	-0.001	0.008
104	150	99.28	1.29	1.99	-0.70	0.427	20.6	0.090	-0.006	-0.017	-0.002	0.010
104	152	100.67	1.14	1.90	-0.76	0.500	19.9	0.090	0.004	0.007	0.002	0.009
104	154	102.28	0.69	1.51	-0.82	0.392	19.4	0.050	-0.003	-0.019	-0.015	0.016
104	156	104.74	0.58	2.40	-1.82	0.388	11.9	0.110	0.003	-0.021	-0.002	0.018
104	158	107.31	0.08	2.42	-2.34	0.398	11.6	0.110	0.005	-0.021	-0.003	0.018
104	160	110.62	-0.18	2.42	-2.60	0.396	10.2	0.110	0.005	-0.019	-0.007	0.020
104	162	114.16	-0.69	2.28	-2.98	0.408	11.3	0.100	0.003	-0.023	-0.009	0.022
104	164	118.62	-0.75	2.28	-3.04	0.408	11.3	0.100	-0.002	-0.022	-0.012	0.022
104	166	123.47	-0.89	2.08	-2.98	0.430	12.1	0.090	-0.004	-0.026	-0.015	0.016
104	168	128.98	-0.82	1.89	-2.72	0.430	12.1	0.080	-0.009	-0.025	-0.017	0.013
104	170	134.80	-0.88	1.98	-2.86	0.432	13.4	0.080	-0.013	-0.026	-0.018	0.008
104	172	141.19	-0.82	1.79	-2.61	0.432	13.4	0.070	-0.015	-0.024	-0.017	0.006
104	174	148.13	-0.62	0.86	-1.48	0.290	0.0	0.000	0.000	0.000	0.009	0.020
104	176	155.51	-0.42	0.81	-1.23	0.280	0.0	0.000	0.000	0.000	0.015	0.015
104	178	163.19	-0.32	0.78	-1.09	0.270	0.0	0.010	0.000	0.000	0.020	0.012
104	180	171.14	-0.35	0.80	-1.16	0.270	0.0	0.010	0.000	0.000	0.024	0.008
104	182	179.41	-0.47	0.80	-1.27	0.260	0.0	0.010	0.000	0.000	0.027	0.005
104	184	187.94	-0.71	0.81	-1.53	0.250	0.0	0.020	0.000	0.000	0.028	0.003
104	186	196.82	-0.98	1.26	-2.24	0.314	30.7	0.030	-0.002	0.001	0.011	-0.004
104	188	205.95	-1.38	1.37	-2.76	0.292	38.1	0.040	0.003	0.000	0.005	-0.003
104	190	215.51	-1.73	0.91	-2.63	0.166	25.0	0.050	0.000	-0.004	0.019	0.004
104	192	225.59	-1.91	1.09	-3.00	0.153	11.3	0.060	0.003	-0.003	0.022	0.004
106	142	113.98	1.25	1.80	-0.55	0.448	23.7	0.100	-0.012	-0.024	0.008	0.004
106	144	112.36	1.13	2.02	-0.88	0.443	25.4	0.100	-0.015	-0.022	0.005	0.004
106	146	111.34	1.04	1.72	-0.67	0.429	27.8	0.070	-0.024	-0.017	-0.003	0.004
106	148	110.99	1.06	1.59	-0.52	0.430	24.8	0.070	-0.025	-0.018	-0.002	0.008
106	150	111.19	1.07	1.37	-0.30	0.416	24.1	0.060	-0.021	-0.014	-0.001	0.009
106	152	111.80	0.96	1.10	-0.15	0.403	23.4	0.040	-0.011	-0.010	-0.005	0.012
106	154	112.96	0.85	2.39	-1.54	0.398	11.6	0.130	0.003	-0.020	0.001	0.006
106	156	114.38	0.49	2.41	-1.92	0.396	10.2	0.130	0.005	-0.018	-0.002	0.008
106	158	116.25	0.07	2.15	-2.07	0.404	8.5	0.120	0.012	-0.018	-0.007	0.012
106	160	118.26	-0.71	1.91	-2.62	0.330	0.0	0.080	0.000	0.000	-0.023	0.040
106	162	121.44	-0.81	1.85	-2.65	0.330	0.0	0.070	0.000	0.000	-0.024	0.043
106	164	125.09	-0.91	1.81	-2.72	0.330	0.0	0.060	0.000	0.000	-0.024	0.046
106	166	129.18	-1.05	1.68	-2.73	0.330	0.0	0.050	0.000	0.000	-0.021	0.047
106	168	133.65	-1.27	1.62	-2.89	0.340	0.0	0.050	0.000	0.000	-0.017	0.046
106	170	138.92	-1.13	1.59	-2.72	0.439	11.8	0.080	-0.011	-0.028	-0.019	0.007
106	172	144.51	-1.12	1.47	-2.59	0.442	13.1	0.070	-0.009	-0.027	-0.019	0.006
106	174	150.85	-0.80	0.92	-1.73	0.300	0.0	-0.010	0.000	0.000	0.012	0.024

Continued. . .

Table 1 contd. . .

Z	N	M_{sp}^{th}	E	E_{mac}	E_{mic}	β_{20}^{sp}	$\gamma^{sp} (^{\circ})$	β_{40}^{sp}	β_{42}^{sp}	β_{44}^{sp}	β_{60}^{sp}	β_{80}^{sp}
106	176	157.50	-0.59	0.87	-1.46	0.290	0.0	-0.010	0.000	0.000	0.017	0.019
106	178	164.60	-0.35	0.94	-1.28	0.280	0.0	-0.020	0.000	0.000	0.022	0.013
106	180	171.88	-0.35	0.84	-1.19	0.270	0.0	-0.010	0.000	0.000	0.026	0.010
106	182	179.51	-0.39	0.82	-1.21	0.260	0.0	-0.010	0.000	0.000	0.027	0.007
106	184	187.39	-0.58	0.68	-1.27	0.240	0.0	0.010	0.000	0.000	0.027	0.006
106	186	195.72	-0.71	1.32	-2.03	0.328	31.3	0.040	-0.007	0.002	0.013	-0.005
106	188	204.16	-1.11	1.21	-2.32	0.323	29.8	0.040	-0.002	0.003	0.010	-0.004
106	190	212.92	-1.56	0.68	-2.25	0.157	26.6	0.040	0.000	-0.004	0.018	0.006
106	192	222.41	-1.65	0.81	-2.46	0.143	12.1	0.050	0.003	-0.004	0.020	0.005
108	144	128.25	0.78	1.30	-0.52	0.434	28.9	0.070	-0.025	-0.016	0.000	0.006
108	146	126.37	0.65	1.28	-0.62	0.429	27.8	0.060	-0.030	-0.017	-0.002	0.010
108	148	125.11	0.58	1.39	-0.81	0.421	28.4	0.050	-0.034	-0.017	-0.005	0.012
108	150	124.66	0.75	1.04	-0.30	0.420	25.4	0.040	-0.029	-0.013	0.000	0.013
108	152	124.87	1.03	1.73	-0.70	0.406	9.9	0.130	0.010	-0.014	-0.001	0.001
108	154	124.76	0.47	1.84	-1.38	0.416	9.7	0.130	0.018	-0.016	-0.003	-0.002
108	156	125.28	-0.01	1.69	-1.71	0.416	9.7	0.120	0.019	-0.019	-0.006	0.004
108	158	126.26	-0.54	1.78	-2.31	0.340	0.0	0.090	0.000	0.000	-0.018	0.041
108	160	128.17	-0.63	1.57	-2.20	0.330	0.0	0.070	0.001	0.000	-0.018	0.045
108	162	130.59	-0.72	1.59	-2.30	0.330	0.0	0.060	0.000	0.000	-0.019	0.049
108	164	133.43	-0.87	1.56	-2.43	0.330	0.0	0.050	0.000	0.000	-0.017	0.051
108	166	136.62	-1.15	1.53	-2.68	0.340	0.0	0.050	0.000	0.000	-0.015	0.050
108	168	140.47	-1.23	1.29	-2.52	0.330	0.0	0.040	0.000	0.000	-0.007	0.047
108	170	144.69	-1.41	1.07	-2.49	0.330	0.0	0.030	0.000	0.000	0.002	0.042
108	172	149.61	-1.33	0.95	-2.28	0.310	0.0	0.000	0.000	0.000	0.012	0.034
108	174	155.36	-0.87	1.03	-1.90	0.300	0.0	-0.020	0.000	0.000	0.018	0.027
108	176	161.30	-0.65	1.01	-1.66	0.290	0.0	-0.020	0.000	0.000	0.024	0.022
108	178	167.63	-0.46	1.01	-1.47	0.280	0.0	-0.020	0.000	0.000	0.028	0.017
108	180	174.31	-0.34	1.00	-1.33	0.270	0.0	-0.020	0.000	0.000	0.031	0.013
108	182	181.08	-0.54	2.01	-2.55	0.400	36.9	0.020	-0.008	-0.018	0.015	-0.010
108	184	188.38	-0.61	2.04	-2.64	0.398	38.9	0.020	-0.005	-0.017	0.009	-0.011
108	186	195.95	-0.79	2.04	-2.83	0.398	38.9	0.030	-0.003	-0.015	0.008	-0.011
108	188	204.01	-0.89	1.91	-2.80	0.384	38.7	0.040	-0.002	-0.012	0.006	-0.010
108	190	212.06	-1.37	0.73	-2.11	0.288	20.3	0.040	-0.004	0.005	0.013	-0.004
108	192	220.92	-1.42	0.60	-2.02	0.146	15.9	0.040	0.004	-0.005	0.018	0.005
110	146	142.96	0.18	1.01	-0.83	0.434	28.9	0.050	-0.034	-0.020	0.001	0.014
110	148	140.92	0.15	1.04	-0.90	0.429	27.8	0.040	-0.038	-0.020	0.002	0.015
110	150	139.72	0.38	0.81	-0.43	0.430	24.8	0.040	-0.035	-0.016	0.007	0.017
110	152	139.16	0.69	1.61	-0.92	0.340	0.0	0.120	0.000	0.000	-0.010	0.020
110	154	138.41	0.27	1.39	-1.12	0.350	0.0	0.110	0.000	0.000	-0.013	0.026
110	156	138.20	-0.13	1.48	-1.61	0.340	0.0	0.100	0.000	0.000	-0.014	0.034
110	158	138.58	-0.47	1.18	-1.65	0.330	0.0	0.070	0.000	0.000	-0.015	0.043
110	160	139.68	-0.62	1.22	-1.84	0.330	0.0	0.070	0.001	0.000	-0.013	0.043
110	162	141.30	-0.73	1.28	-2.01	0.330	0.0	0.060	0.000	0.000	-0.012	0.048
110	164	143.36	-0.90	1.28	-2.18	0.330	0.0	0.040	0.000	0.000	-0.010	0.053
110	166	145.81	-1.17	1.19	-2.36	0.340	0.0	0.040	0.000	0.000	-0.008	0.051
110	168	148.86	-1.30	1.05	-2.36	0.330	0.0	0.030	0.000	0.000	0.001	0.047
110	170	152.36	-1.45	0.97	-2.42	0.320	0.0	0.010	0.000	0.000	0.012	0.042
110	172	156.74	-1.18	1.10	-2.28	0.300	0.0	-0.020	0.000	0.000	0.021	0.034
110	174	161.68	-0.79	1.26	-2.05	0.290	0.0	-0.030	0.000	0.000	0.029	0.027
110	176	166.92	-0.55	1.30	-1.85	0.280	0.0	-0.030	0.000	0.000	0.035	0.023
110	178	172.49	-0.41	1.33	-1.73	0.280	0.0	-0.030	0.000	0.000	0.038	0.019
110	180	178.31	-0.43	1.87	-2.30	0.414	37.2	0.030	-0.006	-0.015	0.019	-0.006
110	182	184.26	-0.74	1.89	-2.63	0.414	37.2	0.030	-0.006	-0.017	0.017	-0.008
110	184	190.85	-0.82	1.84	-2.66	0.405	40.0	0.030	-0.003	-0.009	0.011	-0.009
110	186	197.69	-1.05	1.98	-3.03	0.419	40.2	0.030	0.000	-0.010	0.008	-0.010
110	188	205.04	-1.17	1.17	-2.34	0.402	26.6	0.020	-0.029	-0.008	0.011	-0.011
110	190	212.81	-1.24	0.58	-1.82	0.275	19.1	0.040	-0.003	0.006	0.014	-0.001
110	192	221.00	-1.27	0.43	-1.70	0.148	28.3	0.030	0.000	-0.006	0.015	0.004
112	148	158.71	0.08	0.66	-0.58	0.434	26.0	0.030	-0.040	-0.023	0.013	0.019
112	150	157.02	0.63	0.12	0.52	0.431	21.8	0.030	-0.024	-0.013	0.014	0.023
112	152	155.34	0.63	0.69	-0.06	0.340	0.0	0.100	0.000	0.000	-0.010	0.020
112	154	153.79	0.20	0.70	-0.50	0.340	0.0	0.090	0.000	0.000	-0.012	0.029
112	156	152.75	-0.26	0.72	-0.98	0.340	0.0	0.080	0.000	0.000	-0.012	0.036
112	158	152.43	-0.52	0.67	-1.18	0.330	0.0	0.060	0.000	0.000	-0.010	0.041
112	160	152.82	-0.60	0.76	-1.35	0.330	0.0	0.040	0.000	0.000	-0.009	0.048
112	162	153.62	-0.77	0.88	-1.65	0.330	0.0	0.040	0.000	0.000	-0.007	0.050
112	164	154.93	-0.92	0.93	-1.86	0.330	0.0	0.030	0.000	0.000	-0.003	0.052

Continued. . .

Table 1 contd. . .

Z	N	M_{sp}^{th}	E	E_{mac}	E_{mic}	β_{20}^{sp}	$\gamma^{sp}(\circ)$	β_{40}^{sp}	β_{42}^{sp}	β_{44}^{sp}	β_{60}^{sp}	β_{80}^{sp}
112	166	156.75	-1.07	0.85	-1.92	0.330	0.0	0.020	0.000	0.000	0.003	0.049
112	168	158.91	-1.35	0.82	-2.16	0.330	0.0	0.020	0.000	0.000	0.009	0.046
112	170	162.01	-1.15	1.08	-2.23	0.300	0.0	-0.020	0.000	0.000	0.024	0.037
112	172	165.72	-0.82	1.28	-2.10	0.290	0.0	-0.030	0.000	0.000	0.033	0.031
112	174	169.89	-0.48	1.66	-2.13	0.280	0.0	-0.040	0.000	0.000	0.043	0.025
112	176	174.27	-0.36	1.70	-2.06	0.419	33.3	0.020	-0.023	-0.026	0.024	-0.005
112	178	178.92	-0.42	1.50	-1.92	0.424	34.5	0.030	-0.013	-0.016	0.022	-0.004
112	180	183.77	-0.71	1.53	-2.24	0.424	34.5	0.030	-0.012	-0.017	0.021	-0.007
112	182	189.08	-0.96	1.60	-2.56	0.430	35.6	0.030	-0.010	-0.017	0.018	-0.009
112	184	194.67	-1.33	1.33	-2.66	0.341	58.2	0.010	-0.002	0.000	-0.003	-0.003
112	186	201.15	-1.24	1.13	-2.36	0.316	55.3	0.020	-0.012	0.007	-0.002	-0.003
112	188	208.12	-1.04	0.90	-1.93	0.286	53.6	0.020	-0.011	0.007	-0.001	-0.002
112	190	215.14	-1.19	0.47	-1.65	0.288	20.3	0.040	-0.005	0.010	0.013	-0.001
112	192	222.61	-1.26	0.21	-1.47	0.158	55.3	0.000	-0.003	0.002	0.000	-0.001
114	150	175.66	0.63	-0.35	0.98	0.350	0.0	0.080	0.000	0.000	-0.007	0.015
114	152	172.88	0.32	-0.18	0.50	0.350	0.0	0.080	0.000	0.000	-0.008	0.022
114	154	170.53	-0.12	-0.02	-0.10	0.340	0.0	0.070	0.000	0.000	-0.010	0.029
114	156	168.82	-0.46	0.11	-0.57	0.330	0.0	0.060	0.000	0.000	-0.009	0.034
114	158	167.96	-0.49	0.22	-0.71	0.320	0.0	0.040	0.000	0.000	-0.007	0.040
114	160	167.61	-0.53	0.42	-0.95	0.320	0.0	0.030	0.000	0.000	-0.004	0.046
114	162	167.71	-0.64	0.55	-1.19	0.330	0.0	0.020	0.000	0.000	-0.001	0.050
114	164	168.29	-0.77	0.64	-1.40	0.320	0.0	0.020	0.000	0.000	0.005	0.049
114	166	169.34	-0.93	0.68	-1.61	0.320	0.0	0.010	0.000	0.000	0.013	0.047
114	168	170.99	-0.97	0.91	-1.88	0.310	0.0	-0.010	0.000	0.000	0.024	0.042
114	170	173.46	-0.68	1.28	-1.96	0.290	0.0	-0.030	0.000	0.000	0.036	0.034
114	172	176.37	-0.41	1.70	-2.10	0.290	0.0	-0.040	0.000	0.000	0.046	0.029
114	174	179.71	-0.17	1.66	-1.83	0.270	0.0	-0.030	0.000	0.000	0.051	0.025
114	176	183.20	-0.22	1.13	-1.35	0.433	33.7	0.030	-0.019	-0.015	0.023	-0.003
114	178	186.94	-0.48	1.12	-1.59	0.433	33.7	0.030	-0.016	-0.014	0.022	-0.006
114	180	191.18	-0.67	1.19	-1.85	0.438	34.8	0.030	-0.012	-0.013	0.020	-0.008
114	182	195.27	-1.43	1.34	-2.77	0.444	31.2	0.020	-0.030	-0.026	0.016	-0.013
114	184	199.98	-1.99	1.54	-3.53	0.457	28.8	0.010	-0.040	-0.031	0.012	-0.016
114	186	206.11	-1.54	0.98	-2.53	0.311	56.9	0.020	-0.016	0.013	-0.002	-0.003
114	188	212.45	-1.29	0.98	-2.26	0.300	53.2	0.030	-0.018	0.011	0.000	-0.002
114	190	218.91	-1.31	1.05	-2.36	0.286	36.5	0.060	-0.010	0.015	0.009	0.000
114	192	225.57	-1.53	0.15	-1.68	0.294	17.8	0.030	-0.006	0.007	0.011	-0.005
116	152	191.89	-0.09	-0.69	0.60	0.330	0.0	0.050	0.000	0.000	-0.008	0.023
116	154	188.92	-0.36	-0.44	0.08	0.320	0.0	0.050	0.001	0.001	-0.009	0.027
116	156	186.82	-0.32	-0.32	0.00	0.310	0.0	0.030	0.000	0.000	-0.006	0.032
116	158	185.30	-0.23	-0.10	-0.13	0.310	0.0	0.020	0.000	0.000	-0.003	0.039
116	160	184.22	-0.24	0.10	-0.34	0.310	0.0	0.020	0.000	0.000	0.001	0.043
116	162	183.53	-0.37	0.25	-0.63	0.320	0.0	0.010	0.000	0.000	0.006	0.046
116	164	183.45	-0.41	0.38	-0.79	0.310	0.0	0.010	0.000	0.000	0.014	0.044
116	166	183.71	-0.60	0.55	-1.16	0.310	0.0	0.000	0.000	0.000	0.022	0.043
116	168	184.69	-0.58	0.97	-1.54	0.300	0.0	-0.020	0.000	0.000	0.034	0.038
116	170	186.37	-0.34	1.33	-1.67	0.290	0.0	-0.030	0.000	0.000	0.044	0.033
116	172	188.49	-0.12	1.96	-2.08	0.280	0.0	-0.040	0.000	0.000	0.056	0.028
116	174	191.14	0.16	0.73	-0.58	0.444	35.9	0.030	-0.013	0.006	0.024	-0.003
116	176	193.74	-0.07	0.68	-0.76	0.438	34.8	0.040	-0.011	0.000	0.022	-0.002
116	178	196.71	-0.39	0.70	-1.09	0.438	34.8	0.030	-0.012	-0.003	0.022	-0.006
116	180	200.04	-0.77	0.65	-1.43	0.441	33.0	0.030	-0.018	-0.011	0.018	-0.010
116	182	203.46	-1.51	0.99	-2.50	0.453	30.5	0.020	-0.033	-0.027	0.014	-0.016
116	184	207.88	-1.66	1.09	-2.75	0.453	30.5	0.010	-0.034	-0.026	0.014	-0.019
116	186	212.65	-1.88	1.25	-3.13	0.457	28.8	0.000	-0.040	-0.029	0.010	-0.019
116	188	218.34	-1.59	0.87	-2.46	0.448	29.4	0.010	-0.034	-0.022	0.008	-0.018
116	190	224.42	-1.32	0.46	-1.78	0.286	24.8	0.050	-0.003	0.017	0.013	0.002
116	192	230.30	-1.64	0.00	-1.63	0.301	15.4	0.040	-0.010	0.006	0.013	-0.006
118	154	209.46	-0.01	-0.75	0.74	0.300	0.0	0.030	0.000	0.000	-0.008	0.023
118	156	206.74	0.19	-0.53	0.72	0.290	0.0	0.030	0.000	0.000	-0.004	0.028
118	158	204.35	0.18	-0.40	0.58	0.300	0.0	0.020	0.000	0.000	0.002	0.034
118	160	202.34	0.01	-0.26	0.26	0.310	0.0	0.020	0.000	0.000	0.007	0.039
118	162	200.93	-0.09	-0.10	0.01	0.310	0.0	0.020	0.000	0.000	0.012	0.041
118	164	200.07	-0.15	0.21	-0.35	0.310	0.0	0.000	0.000	0.000	0.022	0.041
118	166	199.60	-0.34	0.50	-0.83	0.310	0.0	-0.010	0.000	0.000	0.030	0.040
118	168	199.82	-0.32	0.85	-1.17	0.300	0.0	-0.020	0.000	0.000	0.039	0.036
118	170	200.85	0.00	0.58	-0.57	0.464	37.1	0.010	-0.021	0.021	0.025	-0.009
118	172	201.99	-0.03	0.60	-0.63	0.464	37.1	0.010	-0.017	0.021	0.024	-0.008

Continued. . .

Table 1 contd. . .

Z	N	M_{sp}^{th}	E	E_{mac}	E_{mic}	β_{20}^{sp}	$\gamma^{sp} (^{\circ})$	β_{40}^{sp}	β_{42}^{sp}	β_{44}^{sp}	β_{60}^{sp}	β_{80}^{sp}
118	174	203.62	-0.05	0.49	-0.54	0.450	36.9	0.020	-0.017	0.014	0.025	-0.007
118	176	205.62	-0.17	0.38	-0.55	0.444	35.9	0.030	-0.013	0.007	0.024	-0.006
118	178	207.91	-0.45	0.39	-0.84	0.444	35.9	0.030	-0.011	0.004	0.022	-0.008
118	180	210.64	-0.73	0.24	-0.97	0.447	34.1	0.030	-0.012	-0.001	0.018	-0.011
118	182	213.46	-1.36	0.44	-1.80	0.453	30.5	0.020	-0.028	-0.023	0.015	-0.018
118	184	217.23	-1.47	0.45	-1.92	0.453	30.5	0.020	-0.026	-0.022	0.014	-0.020
118	186	221.32	-1.68	0.55	-2.23	0.461	29.9	0.010	-0.031	-0.024	0.011	-0.020
118	188	226.19	-1.53	0.39	-1.92	0.453	30.5	0.010	-0.025	-0.018	0.007	-0.019
118	190	231.40	-1.44	0.35	-1.78	0.453	30.5	0.010	-0.025	-0.016	0.004	-0.017
118	192	236.67	-1.70	-0.15	-1.55	0.304	17.3	0.040	-0.008	0.009	0.013	-0.006
120	156	226.20	-1.30	-0.27	-1.02	0.490	39.2	0.040	-0.047	-0.001	0.019	0.002
120	158	223.09	-1.26	-0.20	-1.06	0.492	37.6	0.050	-0.051	-0.001	0.022	0.003
120	160	220.58	-1.17	0.05	-1.22	0.498	38.5	0.040	-0.053	-0.002	0.025	-0.001
120	162	218.76	-0.92	0.18	-1.10	0.498	38.5	0.030	-0.053	0.001	0.026	-0.003
120	164	217.57	-0.57	0.23	-0.80	0.490	39.2	0.030	-0.047	0.009	0.027	-0.005
120	166	216.76	-0.35	0.33	-0.68	0.483	40.0	0.020	-0.041	0.016	0.027	-0.008
120	168	216.40	-0.18	0.33	-0.51	0.469	39.8	0.010	-0.028	0.023	0.026	-0.009
120	170	216.44	-0.10	0.30	-0.40	0.455	39.7	0.010	-0.023	0.023	0.024	-0.009
120	172	216.91	-0.08	0.16	-0.25	0.456	37.9	0.020	-0.017	0.020	0.027	-0.006
120	174	217.83	-0.09	0.08	-0.18	0.450	36.9	0.030	-0.013	0.015	0.027	-0.006
120	176	219.07	-0.25	-0.02	-0.23	0.444	35.9	0.030	-0.008	0.009	0.025	-0.007
120	178	220.69	-0.49	-0.01	-0.48	0.444	35.9	0.020	-0.008	0.006	0.021	-0.010
120	180	222.68	-0.81	0.00	-0.81	0.444	35.9	0.030	-0.006	0.002	0.019	-0.011
120	182	225.12	-1.12	-0.28	-0.83	0.449	32.3	0.020	-0.008	-0.004	0.011	-0.015
120	184	228.07	-1.35	-0.17	-1.19	0.449	32.3	0.020	-0.010	-0.007	0.012	-0.018
120	186	231.42	-1.61	-0.08	-1.53	0.461	29.9	0.010	-0.021	-0.020	0.008	-0.021
120	188	235.58	-1.49	-0.16	-1.32	0.453	30.5	0.010	-0.013	-0.014	0.004	-0.019
120	190	240.11	-1.41	-0.20	-1.22	0.453	30.5	0.010	-0.011	-0.013	-0.001	-0.016
120	192	245.01	-1.36	-0.28	-1.08	0.461	29.9	0.010	-0.011	-0.012	-0.003	-0.014
122	158	244.85	-1.21	-0.57	-0.64	0.497	40.1	0.050	-0.051	-0.002	0.019	0.005
122	160	241.32	-1.37	-0.46	-0.91	0.498	38.5	0.040	-0.059	-0.001	0.023	0.003
122	162	238.77	-1.10	-0.30	-0.80	0.504	39.4	0.040	-0.057	0.002	0.025	0.003
122	164	236.77	-0.81	-0.22	-0.59	0.504	39.4	0.040	-0.054	0.008	0.028	0.003
122	166	235.24	-0.57	-0.06	-0.51	0.497	40.1	0.030	-0.054	0.015	0.026	0.001
122	168	234.43	-0.12	-0.06	-0.06	0.468	41.6	0.020	-0.035	0.021	0.025	-0.006
122	170	233.81	0.04	-0.17	0.21	0.461	40.6	0.020	-0.021	0.022	0.025	-0.006
122	172	233.62	0.11	-0.33	0.44	0.448	38.7	0.020	-0.009	0.018	0.023	-0.004
122	174	233.77	0.06	-0.35	0.40	0.442	37.7	0.010	-0.001	0.013	0.018	-0.005
122	176	234.22	-0.18	-0.39	0.21	0.436	36.6	0.020	0.002	0.007	0.019	-0.006
122	178	235.09	-0.45	-0.32	-0.13	0.436	36.6	0.020	0.003	0.003	0.018	-0.008
122	180	236.33	-0.82	-0.28	-0.55	0.436	36.6	0.030	0.004	-0.001	0.016	-0.010
122	182	238.01	-1.19	-0.22	-0.97	0.436	36.6	0.030	0.004	-0.004	0.014	-0.013
122	184	240.18	-1.51	-0.71	-0.81	0.458	31.6	0.020	-0.001	-0.004	0.007	-0.018
122	186	242.95	-1.67	-0.70	-0.98	0.461	29.9	0.010	-0.009	-0.013	0.004	-0.020
122	188	246.37	-1.61	-0.62	-0.99	0.453	30.5	0.010	-0.002	-0.010	0.000	-0.018
122	190	249.94	-1.81	-0.16	-1.64	0.305	23.2	0.050	-0.001	0.021	0.015	-0.003
122	192	253.87	-2.07	-0.34	-1.72	0.310	20.8	0.050	0.002	0.017	0.010	-0.007
124	160	263.66	-1.48	-1.01	-0.48	0.498	38.5	0.040	-0.064	-0.001	0.021	0.005
124	162	260.38	-1.19	-0.81	-0.39	0.504	39.4	0.050	-0.061	0.002	0.026	0.006
124	164	257.52	-1.01	-0.68	-0.33	0.511	40.3	0.050	-0.057	0.010	0.029	0.007
124	166	255.20	-0.82	-0.52	-0.31	0.503	41.0	0.040	-0.057	0.015	0.026	0.004
124	168	253.79	-0.23	-0.45	0.22	0.482	41.7	0.030	-0.050	0.019	0.023	0.000
124	170	252.72	0.19	-0.74	0.93	0.461	40.6	0.020	-0.012	0.022	0.022	-0.004
124	172	251.77	0.23	-0.71	0.94	0.440	39.5	0.020	0.004	0.015	0.017	-0.001
124	174	251.10	0.07	-0.68	0.76	0.434	38.5	0.020	0.009	0.009	0.016	-0.003
124	176	250.77	-0.23	-0.65	0.42	0.428	37.4	0.030	0.012	0.003	0.016	-0.004
124	178	250.88	-0.56	-0.56	0.00	0.428	37.4	0.030	0.015	0.000	0.012	-0.005
124	180	251.42	-0.92	-0.47	-0.46	0.428	37.4	0.030	0.014	-0.004	0.014	-0.009
124	182	252.41	-1.29	-0.39	-0.91	0.428	37.4	0.040	0.013	-0.006	0.013	-0.011
124	184	253.84	-1.67	-0.46	-1.21	0.436	36.6	0.030	0.010	-0.008	0.010	-0.015
124	186	255.88	-1.87	-1.18	-0.69	0.461	29.9	0.010	-0.001	-0.008	0.001	-0.020
124	188	258.64	-1.78	0.18	-1.96	0.304	27.4	0.070	0.001	0.026	0.016	0.001
124	190	261.43	-2.08	-0.37	-1.71	0.305	23.2	0.050	0.002	0.021	0.015	-0.005
124	192	264.66	-2.37	-0.41	-1.96	0.305	23.2	0.050	0.002	0.020	0.010	-0.006
126	162	283.37	-1.38	-1.48	0.10	0.511	40.3	0.060	-0.059	0.004	0.025	0.007
126	164	279.69	-1.28	-1.35	0.07	0.511	40.3	0.050	-0.060	0.009	0.027	0.006
126	166	276.70	-1.03	-1.09	0.07	0.503	41.0	0.050	-0.057	0.016	0.029	0.005

Continued. . .

Table 1 contd. . .

Z	N	M_{sp}^{th}	E	E_{mac}	E_{mic}	β_{20}^{sp}	$\gamma^{sp}(\circ)$	β_{40}^{sp}	β_{42}^{sp}	β_{44}^{sp}	β_{60}^{sp}	β_{80}^{sp}
126	168	274.31	-0.69	-0.85	0.17	0.496	41.8	0.050	-0.056	0.019	0.028	0.005
126	170	272.82	0.05	-0.91	0.96	0.482	41.7	0.030	-0.050	0.022	0.025	0.002
126	172	271.22	0.16	-0.98	1.14	0.453	41.4	0.020	0.011	0.017	0.012	0.000
126	174	269.79	-0.05	-0.93	0.89	0.426	39.3	0.030	0.016	0.006	0.012	-0.001
126	176	268.64	-0.46	-1.03	0.56	0.422	36.3	0.030	0.018	0.001	0.014	-0.005
126	178	268.05	-0.79	-0.84	0.05	0.428	37.4	0.030	0.020	-0.003	0.012	-0.007
126	180	267.88	-1.16	-0.73	-0.43	0.428	37.4	0.030	0.020	-0.007	0.012	-0.010
126	182	268.19	-1.52	-0.63	-0.89	0.428	37.4	0.030	0.021	-0.009	0.009	-0.011
126	184	269.02	-1.80	-0.46	-1.33	0.426	39.3	0.040	0.018	-0.008	0.009	-0.012
126	186	270.62	-1.76	-0.03	-1.73	0.304	27.4	0.070	0.002	0.028	0.019	0.001
126	188	272.22	-2.15	-0.37	-1.78	0.309	24.9	0.060	0.004	0.025	0.015	-0.003
126	190	274.31	-2.49	-0.70	-1.79	0.314	22.5	0.050	0.003	0.022	0.012	-0.009
*126	192	276.92	-2.72	-0.46	-2.26	0.305	23.2	0.060	0.005	0.022	0.008	-0.008

* marginally unbound nucleus

References

- [1] Yu. Ts. Oganessian et al., *Phys. Rev. Lett.* **83**, 3154 (1999).
- [2] Yu. Ts. Oganessian et al., *Nature* (London) **400**, 242 (1999).
- [3] Yu. Ts. Oganessian et al., *Phys. Rev. C*, **62**, 041604 (2000).
- [4] Yu. Ts. Oganessian et al., *Phys. Rev. C*, **63**, 011301(R)(2001).
- [5] Yu. Ts. Oganessian et al., *Phys. Rev. C*, **69**, 054607 (2004).
- [6] Yu. Ts. Oganessian et al., *Phys. Rev. Lett.* **104**, 142502 (2010).
- [7] Yu. Ts. Oganessian et al., *Phys. Rev. C* **74**, 044602 (2006).
- [8] Yu. Ts. Oganessian et al., *Phys. Rev. C* **79**, 024603 (2009).
- [9] Yu. Ts. Oganessian et al., *Phys. Rev. Lett.*, **104**, 142502 (2010).
- [10] Yu. Ts. Oganessian et al., *Phys. Rev. C* **83**, 054315 (2011).
- [11] Yu. Ts. Oganessian et al., *Phys. Rev. Lett.* **108**, 022502 (2012).
- [12] Ch. E. Düllmann et al., *Phys. Rev. Lett.* **104**, 252701 (2010).
- [13] L. Stavsetra et al., *Phys. Rev. Lett.* **103**, 132502 (2009).
- [14] G. Münzenberg et al., *Z. Phys. A* **333**, 163-175, (1989).
- [15] G. Münzenberg et al., *Z. Phys. A* **324**, 489-490, (1986).
- [16] G. Münzenberg et al., *Z. Phys. A* **315**, 145-158, (1984).
- [17] S. Hofmann and G. Münzenberg *Rev. Mod. Phys.*, **72**, 733-767 (2000).
- [18] S. Hofmann et al., *Z. Phys. A* **350**, 281-282, (1995).
- [19] S. Hofmann *Nuclear Physics News* 5, 28, (1995).
- [20] S. Hofmann et al., *Z. Phys. A*, **350**, 277(1995).
- [21] S. Hofmann et al., *Z. Phys. A*, **354**, 229-230, (1996).
- [22] S. Hofmann et al., *Z. Phys. A*, 14, 147 (2002).
- [23] S. Hofmann et al., *Eur.Phys.J. A*, **32**, 251 (2007).
- [24] G. Audi et al., *Nucl. Phys. A* 729 (2003) 1.
- [25] G. Audi, A.H. Wapstra, and C. Thibault (2003) *Nucl. Phys. A*729, 337.
- [26] S. Goriely, M. Samyn, and J.M. Pearson, (2007) *Phys. Rev. C*75, 064312.
- [27] P. Möller, J.R. Nix, W.D. Myers and W.J. Świątecki, *At. Data Nucl. Data Tables* **59** (1995) 185.
- [28] J. Duflo and A.P. Zuker (1995) *Phys. Rev. C*52, 23.
- [29] J. Duflo and A.P. Zuker (1996) at <http://csn-srv3.in2p3.fr/AMDC/theory>.
- [30] P. Reiter et al., *Phys. Rev. Lett.* **82**, 509512 (1999).
- [31] S. Ćwiok et al., *Nucl. Phys. A* **420**, 254 (1983).
- [32] G. Leander et al., Proc Int. Conf. AMCO 7-1984, O. Klepper (ed.) TH-Darmstad p.466.
- [33] K. Boning, Z. Patyk, A. Sobiczewski, S. Ćwiok, *Z. Phys.A* **325**, 479 (1986).
- [34] A. Sobiczewski, Z. Patyk, S. Ćwiok *Z. Phys.A* **186**, 6 (1987).

- [35] S. Ówiok, J. Dobaczewski, P.-H. Heenen, P. Magierski and W. Nazarewicz, *Nucl. Phys. A* **611**, 211 (1996).
- [36] S. Ówiok, P.-H. Heenen, W. Nazarewicz, *Nature* **433**, 709 (2005).
- [37] A. Baran, Z. Lojewski, K. Sieja, and M. Kowal, *Phys. Rev. C* **72**, 044310 (2005).
- [38] K. Siwek-Wilczynska, T. Cap, M. Kowal, A. Sobiczewski, and J. Wilczyński, *Phys. Rev. C*, submitted (2012).
- [39] K. Blaum, *Physics Reports*, 425 (2006) 1.
- [40] D. Lunney, J.M. Pearson, C. Thibault, *Rev. Mod. Phys.* **75** (2003) 1021.
- [41] H.J. Krappe, J.R. Nix and A.J. Sierk, *Phys. Rev. C* **20** (1979) 992.
- [42] I. Muntian, Z. Patyk and A. Sobiczewski, *Acta Phys. Pol. B* **32**, 691 (2001).
- [43] P. Möller and J.R. Nix, *Nucl. Phys. A* **361** (1981) 117; *At. Data Nucl. Data Tables* **26** (1981) 165.
- [44] V.M. Strutinsky *Nucl. Phys. A* **95** (1967) 420.
- [45] V.M. Strutinsky *Nucl. Phys. A* **122** (1968) 1.
- [46] D. G. Madlanmd and J. R. Nix, *Nucl. Phys A*, 476, 1, (1998).
- [47] S. Ówiok, J. Dudek, W. Nazarewicz, J. Skalski and T. Werner, *Comput. Phys. Commun.* **46** (1987) 379.
- [48] J. Bardeen, L.N. Cooper and J.R. Schrieffer, *Phys. Rev.* **108** (1957) 1175.
- [49] R. W Hasse, W. D. Myers, "Geometrical Relationships of Macroscopic Nuclear Physics." *Springer-Verlag Berlin Heidelberg*, (1988).
- [50] P. Möller, R. Bengtsson, B. G. Carlsson, P. Olivius, and T. Ichikawa, *Phys. Rev. Lett.* **97**, 162502 (2006).
- [51] P. Jachimowicz, M. Kowal, P. Rozmej, J. Skalski and A. Sobiczewski, *Int. J. Mod. Phys. E***18**, **4**, 1088 (2009).
- [52] P. Jachimowicz, M. Kowal, P. Rozmej, J. Skalski and A. Sobiczewski, *Int. J. Mod. Phys. E***19**, **4**, 768 (2010).
- [53] P. Jachimowicz, M. Kowal, P. Rozmej, J. Skalski and A. Sobiczewski, *Int. J. Mod. Phys. E***20**, **2**, 514 (2011).
- [54] P. Jachimowicz, M. Kowal, J. Skalski, *Int. J. Mod. Phys. E***19**, 508 (2010).
- [55] R. E. Bellman, R. E. Kalaba, "Quasilinearization and nonlinear boundary value problems", American Elsevire, New York, (1965).
- [56] A. Baran, K. Pomorski, A. Lukasiak and A. Sobiczewski, *Nucl. Phys. A* **361**, (1981).
- [57] S. Ówiok and A. Sobiczewski, *Z. Phys. A* **342**, (1992).
- [58] R. A. Gherghescu, J. Skalski, Z. Patyk and A. Sobiczewski, *Nucl. Phys. A* **651**, (1999).
- [59] V. Luc and P. Soille, *IEEE Trans. Pattern Anal. Mach. Intell.*, **13**, 583 (1991).
- [60] A. Mamdough, J.M. Pearson, M. Rayet, and F. Tondeur, *Nucl. Phys. A* **644**, 389 (1998).
- [61] B. Hayes, *Am. Sci.* **88**, 481 (2000).
- [62] P. Möller, A. J. Sierk and A. Iwamoto, *Phys. Rev. Lett.* **92**, 072501 (2004).
- [63] P. Möller, A. J. Sierk, T. Ichikawa, A. Iwamoto, R. Bengtsson, H. Uhrenholt, and S. Åberg, *Phys. Rev. C* **79**, 064304 (2009).
- [64] R. Capote et. al. Nuclear Data Sheets 110 (2009) 31073214, <http://www-nds.iaea.org/RIPL-3/>.
- [65] P. Jachimowicz, M. Kowal, J. Skalski, *Phys. Rev. C* **83**, 054302, (2011).
- [66] M. Kowal, P. Jachimowicz, A. Sobiczewski, *Phys. Rev. C* **82**, 014303, (2010).
- [67] A. Dobrowolski, K. Pomorski, and J. Bartel, *Phys. Rev. C* **75**, 024613 (2007).
- [68] H. Abusara, A. V. Afanasjev, and P. Ring *Phys. Rev. C* **82**, 044303, (2010).
- [69] H. Abusara, A. V. Afanasjev, and P. Ring *Phys. Rev. C* **85**, 024314, (2012).
- [70] J. Erler, K. Langanke, H. P. Loens, G. Martnez-Pinedo, and P.-G.Reinhard *Phys. Rev. C* **85**, 025802, (2012).
- [71] R. Smolanczuk, J. Skalski and A. Sobiczewski: *Phys. Rev. C* **52**, 1871 (1995).